Path-Dependent Volatility and the Conditional Performance of Equity Factors

Bernd J. Wuebben
AllianceBernstein, New York
`bernd.wuebben@alliancebernstein.com`

January 3, 2026

Abstract

The performance of equity factor strategies depends not only on the level of market volatility but on the multi-scale path by which that volatility formed. I introduce *multi-scale path states*, a low-dimensional representation of recent return and volatility dynamics across horizons that distinguishes abrupt crash-driven volatility spikes from slowly accumulating stress regimes. Using six decades of U.S. equity data, I document four main findings. First, factor returns and higher moments differ sharply across path states, even after controlling for volatility levels: momentum earns 1.4% monthly in calm states but loses 3.9% in crash-spike states, while quality exhibits the opposite pattern. Second, cross-sectional signal efficacy varies significantly with path states— momentum information coefficients turn negative during rapid volatility expansions, indicating that predictability itself is regime-dependent. Third, factor crashes are heavily concentrated in crash-spike states: nearly half of all momentum crashes occur in a regime that comprises just 7% of the sample. Fourth, a parsimonious state-conditioned exposure rule that reduces factor exposure during crash-spike states improves out-of-sample Sharpe ratios by 15–40%, reduces maximum drawdowns by 25–50%, and lowers turnover relative to naive volatility-scaling approaches. I interpret these findings through three economic channels: arbitrage capital dynamics and deleveraging, information revelation and signal efficacy, and crowding amplification. The results suggest that factor premia are best understood as compensation for *path-conditional risk*—risk that depends not merely on how volatile markets are, but on how they became so.

Keywords: Factor investing, momentum crashes, volatility regimes, path dependence, multi-scale analysis, risk management, limits to arbitrage

JEL Classification: G11 (Portfolio Choice; Investment Decisions), G12 (Asset Pricing; Trading Volume; Bond Interest Rates), G14 (Information and Market Efficiency), G17 (Financial Forecasting and Simulation)

Contents

1 Introduction

Equity factor premia—the excess returns earned by portfolios sorted on characteristics such as momentum, value, quality, and low risk—are among the most robust findings in empirical finance. These premia have been documented across asset classes, geographies, and time periods spanning more than a century [Fama & French, 1993; Asness et al., 2013; Hou et al., 2020]. Yet despite their long-run statistical reliability, factor strategies remain difficult to deploy at institutional scale. Factor portfolios experience prolonged drawdowns, episodic crashes, and regime-dependent performance reversals that challenge their suitability for investors with finite horizons and binding risk constraints.

The fragility of factor investing is nowhere more evident than in the behavior of momentum. The momentum premium—buying past winners and selling past losers—has been called "the premier anomaly" for its robustness and economic magnitude [Fama & French, 2008]. Yet momentum strategies have experienced catastrophic losses precisely when investors could least afford them: in the aftermath of the 1932 market bottom, during the 2009 recovery, and in the violent reversals of March 2020. These "momentum crashes" [Daniel & Moskowitz, 2016] can erase years of accumulated gains in a matter of weeks.

A natural response to factor fragility is to condition on market volatility. When volatility is high, factor strategies are risky; prudent investors should reduce exposure. This intuition underlies the widespread practice of volatility scaling and the academic literature on conditional factor models [Moreira & Muir, 2017]. Yet volatility-based conditioning, while helpful, remains incomplete. Two market environments with identical volatility levels can have profoundly different implications for factor risk and return, depending on the *path* by which volatility formed.

Consider two hypothetical scenarios, both characterized by annualized market volatility of 25%. In the first, volatility has risen from 12% to 25% over the past week following an unexpected shock—a sudden crash, a geopolitical event, or a liquidity crisis. In the second, volatility has drifted upward from 18% to 25% over several months amid persistent macroeconomic uncertainty. Standard volatility conditioning treats these environments as equivalent. But an investor in the first scenario faces margin calls, forced deleveraging, and the prospect of correlated position unwinds across the arbitrage community. An investor in the second faces elevated but manageable risk, with time to adjust positions and access to functioning markets.

This paper argues that the distinction between these scenarios—the *path* of volatility formation— is central to understanding factor performance. I introduce *multi-scale path states*, a compact representation of recent market dynamics that captures not only the level of volatility but also the speed, persistence, and multi-horizon structure of volatility formation. By distinguishing crash-driven spikes from gradual stress accumulation, path states identify market environments with qualitatively different implications for factor investing.

The construction of path states draws on insights from the volatility modeling literature, particularly the recent work on "rough" volatility and multi-scale price dynamics [Gatheral et al., 2018; Morel et al., 2024]. Financial return processes exhibit scale-dependent structure: short-horizon volatility responds rapidly to shocks, while longer-horizon volatility reflects accumulated stress and regime persistence. The ratio of short-horizon to long-horizon realized volatility provides a simple but powerful signal of volatility acceleration or deceleration—a signal that distinguishes between qualitatively different market regimes.

Using monthly U.S. equity returns from 1963 to 2023, I document four main findings.

First, factor returns and higher moments differ dramatically across path states, even after controlling for volatility levels. Momentum earns an average monthly return of 1.4% in calm, trending markets but loses 3.9% in crash-spike states—a swing of over 60 percentage points annualized. Value

displays more modest but still significant state dependence, with losses concentrated in crash-spike states and strong performance in recoveries. Quality and low-risk factors exhibit the opposite pattern, providing positive returns and defensive properties precisely when momentum and value suffer.

Second, the efficacy of factor signals—as measured by cross-sectional information coefficients (ICs)—varies sharply across path states. Momentum ICs are strongly positive in calm markets but turn *negative* in crash-spike states, indicating that past winners become future losers. This IC reversal is the cross-sectional signature of momentum crashes. Quality ICs, by contrast, are highest during market stress, consistent with flight-to-quality dynamics.

Third, factor crashes are heavily concentrated in specific path states. Nearly half of all momentum crashes (defined as monthly returns below the 5th percentile) occur in crash-spike states, which comprise just 7% of the sample. The conditional probability of a momentum crash given a crash-spike state exceeds 33%—more than six times the unconditional crash probability. Identifying these states in real time offers the prospect of avoiding the worst factor outcomes.

Fourth, a parsimonious state-conditioned exposure rule materially improves out-of-sample factor performance. By reducing or eliminating momentum exposure in crash-spike states, investors can improve Sharpe ratios by 15–40%, reduce maximum drawdowns by 25–50%, and avoid the catastrophic crashes that have historically derailed momentum strategies. Importantly, this improvement comes with lower turnover than standard volatility-scaling approaches, as path states are more persistent than volatility levels.

I interpret these findings through three economic channels. The first is *arbitrage capital dynamics*: when volatility spikes rapidly, binding funding constraints force simultaneous deleveraging across the arbitrage community, generating correlated selling pressure and factor crashes. The second is *information revelation*: in crash-spike states, prices are driven by liquidity demand rather than fundamental information, severing the link between factor signals and future returns. The third is *crowding amplification*: as factor strategies have become institutionalized, position similarity has increased, amplifying crash dynamics when crowded positions unwind together.

These mechanisms suggest that factor premia are best understood as compensation for *path-conditional risk.* The unconditional factor premium is a weighted average across market regimes, including periods of large losses. Investors who can identify path states in real time—or who have longer horizons and greater tolerance for drawdowns—can capture higher risk-adjusted returns by conditioning their exposure on how volatility formed, not merely on its level.

The remainder of the paper proceeds as follows. Section 2 reviews the related literature on factor investing, volatility modeling, and conditional asset pricing. Section 3 describes the data and factor construction. Section 4 develops the multi-scale path state methodology, defining the state vector and regime classification. Section 5 presents the core empirical results on conditional factor performance. Section 6 describes the state-conditioned portfolio construction and out-of-sample performance. Section 7 develops the economic interpretation and presents supporting evidence for the proposed channels. Section 8 conducts robustness tests. Section 9 concludes.

2   Related Literature

This paper connects several strands of the finance literature: the documentation and explanation of equity factor premia, the modeling of volatility dynamics, and the study of conditional asset pricing and factor timing.

2.1 Equity Factor Premia

The existence of cross-sectional return predictability based on firm characteristics is one of the most extensively documented findings in empirical finance. Fama & French [1993] established the modern factor framework with their three-factor model incorporating market, size, and value factors. Jegadeesh & Titman [1993] and Carhart [1997] documented the momentum premium, showing that stocks with high past returns continue to outperform. Subsequent work has identified dozens of additional characteristics that predict returns, leading to concerns about data mining [Harvey et al., 2016; McLean & Pontiff, 2016] and efforts to identify a parsimonious set of robust factors [Hou et al., 2015; Fama & French, 2015; Stambaugh & Yuan, 2017].

Despite their statistical robustness, factor premia exhibit substantial time variation. Fama & French [1989] showed that expected returns vary with business cycle indicators. Chordia et al. [2014] documented declining profitability of anomalies over time, potentially reflecting increased arbitrage activity. Arnott et al. [2016] raised concerns about "factor timing" based on valuation spreads.

My contribution to this literature is to show that factor performance depends not only on macroeconomic conditions or factor valuations but on the *path dynamics* of market volatility. This finding suggests that factor premia reflect compensation for a specific form of risk—path-conditional risk—that is not captured by standard conditioning variables.

2.2 Momentum Crashes

The vulnerability of momentum to crashes has received particular attention. Daniel & Moskowitz [2016] provide a comprehensive analysis of momentum crashes, documenting their concentration in market rebounds following crashes and developing a model based on time-varying factor loadings. Barroso & Santa-Clara [2015] show that momentum crashes are partially predictable using realized volatility and propose a volatility-scaled momentum strategy that improves risk-adjusted returns. Daniel et al. [2012] link momentum crashes to investor overconfidence and delayed overreaction.

My analysis differs from this literature in emphasizing the *multi-scale path* of volatility rather than its level. While Barroso & Santa-Clara [2015] scale momentum exposure inversely with realized volatility, I show that the path by which volatility formed—specifically, whether it arrived via a sudden spike or gradual accumulation—contains additional information about crash risk. Two periods with identical realized volatility can have very different implications for momentum, depending on the volatility path.

2.3 Volatility Modeling and Multi-Scale Dynamics

The volatility literature has long recognized that volatility exhibits complex temporal dynamics. Engle [1982] introduced ARCH models to capture volatility clustering. Bollerslev [1986] extended this framework with GARCH. More recently, Gatheral et al. [2018] documented "rough" volatility dynamics, showing that volatility exhibits rougher sample paths than standard diffusion models imply, with important implications for option pricing and volatility forecasting.

Morel et al. [2024] develop a "Path Shadowing Monte Carlo" method that exploits multi-scale volatility structure for prediction. Their approach uses Scattering Spectra—wavelet-based statistics that capture dependencies across time scales—to generate realistic price paths and condition on observed history. My path-state construction can be viewed as a simplified, economically-motivated version of their multi-scale representation, tailored for the application to factor timing rather than volatility prediction.

The insight that short-horizon and long-horizon volatility contain different information is central to my approach. The ratio of short-horizon to long-horizon realized volatility—what I call the

"volatility ratio"—captures the speed of volatility formation. A high ratio indicates recent volatility acceleration (a spike); a low ratio indicates volatility decay (normalization). This ratio provides information about market dynamics beyond what is captured by volatility levels alone.

2.4 Conditional Asset Pricing and Factor Timing

The literature on conditional asset pricing examines how risk and expected returns vary with state variables. Jagannathan & Wang [1996] and Lettau & Ludvigson [2001] condition on business cycle variables. Santos & Veronesi [2006] use labor income and consumption-wealth ratios. Boguth et al. [2011] examine conditioning information in the context of mutual fund performance evaluation.

Factor timing—adjusting factor exposure based on predictive signals—has generated controversy. Asness et al. [2017] argue that factor timing is difficult in practice, with limited out-of-sample evidence of success. Moreira & Muir [2017] propose volatility-managed portfolios that scale factor exposure inversely with conditional variance, documenting improved Sharpe ratios. Cederburg et al. [2020] and Liu et al. [2019] provide critical assessments of volatility timing.

My approach differs from standard factor timing in several respects. First, I condition on the path of volatility formation rather than its level, providing incremental information beyond volatility scaling. Second, my conditioning is parsimonious and designed to avoid overfitting: the regime classification uses fixed thresholds based on economic intuition rather than statistically optimized cutoffs. Third, I focus on crash avoidance—identifying states where factor exposure should be reduced to zero—rather than continuous timing. This conservative approach sacrifices some potential gains but reduces the risk of overfitting and transaction costs.

2.5 Limits to Arbitrage and Funding Liquidity

The economic interpretation of my findings draws on the limits-to-arbitrage literature. Shleifer & Vishny [1997] formalize the idea that arbitrage is risky and capital-constrained. Gromb & Vayanos [2010] survey the literature on financially constrained arbitrage. Brunnermeier & Pedersen [2009] model liquidity spirals in which losses lead to deleveraging, which leads to further losses.

Koijen & Yogo [2018] document that institutional crowding—the tendency of investors to hold similar positions—amplifies price dislocations. When many investors hold similar factor positions, forced selling by some triggers margin calls and redemptions for others, creating correlated selling pressure. This crowding channel helps explain why factor crashes are concentrated in periods of rapid volatility expansion, when funding constraints bind across the arbitrage community.

2.6 Relationship to Path-Dependent Volatility Models

Recent work by Guyon & Lekeufack [2023] develops "path-dependent volatility" models in which current volatility depends on the path of past returns and past squared returns. These models capture important stylized facts about volatility dynamics, including the leverage effect and the "Zumbach effect." My path-state construction shares the intuition that history matters for current market dynamics, but applies this insight to factor returns rather than volatility itself.

Morel et al. [2024] show that path-dependent representations outperform traditional models for volatility forecasting and option pricing. My results extend this finding to the domain of cross-sectional factor returns: the path of market volatility predicts not only future volatility but also the cross-sectional performance of factor strategies.

2.7 Contribution

My contribution relative to this literature is threefold.

Conceptually, I show that factor premia are best understood as compensation for path-conditional risk. The relevant conditioning variable is not merely the level of volatility but the multi-scale path by which volatility formed. This perspective unifies several previously distinct phenomena—momentum crashes, flight-to-quality, and factor correlation dynamics—under a common framework.

Empirically, I provide systematic evidence that path states explain variation in factor returns, signal efficacy, and crash risk beyond what is captured by volatility levels or standard macroeconomic conditioning variables. The state-conditional variation is economically large: the difference in expected momentum returns between calm and crash-spike states exceeds 60 percentage points annualized.

Practically, I demonstrate that path-state conditioning can be implemented in real time using publicly available data, with material improvements in out-of-sample performance. The state-conditioned approach achieves higher Sharpe ratios and lower drawdowns than either unconditional factor investing or standard volatility scaling, with lower turnover than volatility-based approaches.

3 Data

This section describes the data sources, sample construction, factor definitions, and transaction cost assumptions used throughout the paper.

3.1 Equity Returns and Universe

3.1.1 Data Sources

Stock returns and pricing data are obtained from the Center for Research in Security Prices (CRSP) Monthly Stock File. I use monthly holding-period returns that include dividends and adjust for stock splits, rights offerings, and other capital events. Daily returns from CRSP are used to compute realized volatility measures and path-state variables.

Accounting data are obtained from the Compustat North America Fundamentals Annual File. I match Compustat and CRSP using the standard CRSP-Compustat Merged (CCM) linking table, requiring a valid link throughout the fiscal year.

Market-level data, including the S&P 500 index level and the risk-free rate, are obtained from CRSP and Kenneth French's data library. The market return is the value-weighted return on all CRSP stocks. The risk-free rate is the one-month Treasury bill rate.

3.1.2 Sample Period

The sample period spans January 1963 through December 2023, yielding 732 months of data. The start date of 1963 reflects the availability of reliable Compustat data and is standard in the empirical asset pricing literature. The end date represents the most recent data available at the time of analysis.

For out-of-sample tests, I split the sample into a training period (January 1963 through December 1999) and an evaluation period (January 2000 through December 2023). All portfolio construction rules, regime thresholds, and model parameters are estimated using only training-period data. Results reported for the evaluation period are strictly out-of-sample.

3.1.3 Universe Construction

The baseline universe consists of all common stocks listed on the New York Stock Exchange (NYSE), American Stock Exchange (AMEX), and NASDAQ. I apply the following filters:

1. **Share type**: Include only common stocks (CRSP share codes 10 and 11). This excludes ADRs, REITs, closed-end funds, units, and other non-common equity.

2. **Exchange**: Include stocks listed on NYSE (exchange code 1), AMEX (exchange code 2), and NASDAQ (exchange code 3).

3. **Price filter**: Exclude stocks with end-of-month prices below \$1. This filter mitigates microstructure noise and bid-ask bounce effects that disproportionately affect very low-priced stocks.

4. **Size filter**: Exclude stocks with market capitalization below the 20th percentile of NYSE-listed stocks. This filter removes microcap stocks, which are difficult to trade in practice and can dominate equal-weighted portfolios. Following Fama & French [2008], I use NYSE breakpoints to avoid the filter being overwhelmed by small NASDAQ stocks.

5. **Return history**: Require at least 12 months of non-missing return data prior to portfolio formation. This ensures sufficient data for computing momentum signals and other characteristics.

6. **Delisting returns**: Incorporate delisting returns from CRSP to avoid survivorship bias. When a stock delists and the delisting return is missing, I follow Shumway [1997] and assume a delisting return of -30% for performance-related delistings (delisting codes 500 and 520–584) and zero otherwise.

After applying these filters, the universe averages approximately 2,800 stocks per month over the full sample. The universe has grown over time, from roughly 1,500 stocks in the 1960s to over 3,500 in recent years, reflecting the expansion of public equity markets and the growth of NASDAQ.

Table 1 provides summary statistics for the universe.

3.2 Factor Signal Definitions

I construct four canonical factor signals representing momentum, value, quality, and low risk. Each signal is computed at the end of each month t using only information available at that time.

3.2.1 Momentum

The momentum signal follows Jegadeesh & Titman [1993] and Carhart [1997]. For each stock i at the end of month t, the momentum signal is the cumulative return from month $t-12$ through month $t-2$:

$$\text{MOM}_{i,t} = \prod_{s=t-12}^{t-2} (1 + r_{i,s}) - 1 \tag{1}$$

where $r_{i,s}$ is the return on stock i in month s. The most recent month ($t-1$ to t) is skipped to avoid the short-term reversal effect documented by Jegadeesh [1990].

Stocks with fewer than 8 non-missing monthly returns during the formation period are excluded from the momentum sort. This requirement ensures that the momentum signal reflects a reasonably complete return history.

Table 1: Universe Summary Statistics

	Mean	**Std Dev**	**P10**	**P50**	**P90**
Panel A: Universe Size					
Number of stocks	2,812	684	1,842	2,756	3,685
Panel B: Stock Characteristics (Cross-Sectional Averages)					
Market cap ($ millions)	4,285	8,124	142	892	12,450
Monthly return (%)	1.12	5.82	−8.45	0.85	10.92
Book-to-market	0.72	0.48	0.22	0.58	1.45
12-1 month return (%)	14.8	42.5	−32.5	10.2	68.4
Gross profitability	0.32	0.22	0.08	0.28	0.62
60-month beta	1.08	0.52	0.45	1.02	1.78

Notes: Table reports summary statistics for the stock universe. Panel A shows the time series of universe size. Panel B shows cross-sectional averages of stock characteristics, pooled across all months. Market capitalization is in millions of dollars. Book-to-market is the ratio of book equity to market equity. 12-1 month return is cumulative return from month $t-12$ to $t-2$. Gross profitability is revenues minus cost of goods sold, divided by total assets. 60-month beta is estimated from a regression of monthly stock returns on market returns over the prior 60 months. Sample period is January 1963 to December 2023.

3.2.2 Value

The value signal follows Fama & French [1993]. For each stock i at the end of month t, the value signal is the book-to-market ratio:

$$\text{VAL}_{i,t} = \frac{\text{BE}_{i,\tau}}{\text{ME}_{i,t}} \tag{2}$$

where $\text{BE}_{i,\tau}$ is book equity for the fiscal year ending in calendar year τ and $\text{ME}_{i,t}$ is market equity at the end of month t.

Following standard conventions, I use book equity from the fiscal year ending in calendar year $t-1$ matched with market equity from December of year $t-1$ to form portfolios from July of year t through June of year $t+1$. This timing convention ensures that accounting data are publicly available before being used and allows for the typical reporting lag in financial statements.

Book equity is defined as stockholders' equity, plus deferred taxes and investment tax credit, minus preferred stock. Stockholders' equity is measured as Compustat item `SEQ`; if missing, I use common equity (`CEQ`) plus preferred stock par value (`PSTK`); if still missing, I use total assets (`AT`) minus total liabilities (`LT`). Deferred taxes are measured as `TXDITC`; if missing, I use deferred taxes (`TXDB`) plus investment tax credit (`ITCB`). Preferred stock is measured as redemption value (`PSTKRV`); if missing, I use liquidating value (`PSTKL`); if still missing, I use par value (`PSTK`).

Stocks with negative book equity are excluded from the value sort.

3.2.3 Quality

The quality signal follows Novy-Marx [2013]. For each stock i at the end of month t, the quality signal is gross profitability:

$$\text{QUAL}_{i,t} = \frac{\text{REVT}_{i,\tau} - \text{COGS}_{i,\tau}}{\text{AT}_{i,\tau}} \tag{3}$$

where $\text{REVT}_{i,\tau}$ is total revenue, $\text{COGS}_{i,\tau}$ is cost of goods sold, and $\text{AT}_{i,\tau}$ is total assets, all from the fiscal year ending in calendar year τ.

The same timing convention as for value is used: accounting data from fiscal year $t-1$ are matched with market data from December of year $t-1$ to form portfolios from July of year t through June of year $t+1$.

Stocks with missing revenue, cost of goods sold, or total assets are excluded from the quality sort. Financial firms (SIC codes 6000–6999) are excluded from the quality sort because their profitability measures are not comparable to those of non-financial firms.

3.2.4 Low Risk

The low-risk signal follows Frazzini & Pedersen [2014]. For each stock i at the end of month t, the low-risk signal is the negative of market beta:

$$\text{LVOL}_{i,t} = -\hat{\beta}_{i,t} \tag{4}$$

where $\hat{\beta}_{i,t}$ is estimated from a regression of monthly stock excess returns on market excess returns over the prior 60 months:

$$r_{i,s} - r_{f,s} = \alpha_i + \beta_i(r_{m,s} - r_{f,s}) + \varepsilon_{i,s}, \quad s \in \{t - 60, \ldots, t - 1\} \tag{5}$$

The negative sign ensures that high values of the signal correspond to low-risk stocks, maintaining consistency with the other factors (where high signal values indicate the "long" side of the factor).

Stocks with fewer than 36 non-missing monthly returns during the estimation period are excluded from the low-risk sort. To reduce noise in beta estimates, I winsorize estimated betas at the 1st and 99th percentiles of the cross-sectional distribution each month.

3.3 Factor Portfolio Construction

3.3.1 Sorting Procedure

At the end of each month t, I sort stocks into decile portfolios based on each factor signal. The sorting procedure is as follows:

1. Compute the factor signal for all stocks in the universe with non-missing data.

2. Determine decile breakpoints using only NYSE-listed stocks. This ensures that each decile contains a comparable number of NYSE stocks and prevents the extreme deciles from being dominated by small NASDAQ stocks.

3. Assign all stocks (NYSE, AMEX, and NASDAQ) to deciles based on the NYSE breakpoints.

4. Compute value-weighted returns for each decile portfolio over month $t+1$.

3.3.2 Factor Return Computation

The factor return in month $t+1$ is the return difference between the extreme decile portfolios:

$$r_{t+1}^f = r_{t+1}^{\text{D10}} - r_{t+1}^{\text{D1}} \tag{6}$$

where D10 is the top decile (highest signal values) and D1 is the bottom decile (lowest signal values).

For momentum, value, and quality, D10 contains stocks expected to outperform (past winners, cheap stocks, profitable stocks) and D1 contains stocks expected to underperform. For low risk, the sign convention is reversed: D10 contains low-beta stocks (expected to outperform on a risk-adjusted basis) and D1 contains high-beta stocks.

3.3.3 Rebalancing

Portfolios are rebalanced monthly at the end of each month. For value and quality, which use annual accounting data, the underlying signals change only once per year (in June), but portfolio weights are updated monthly to reflect changes in market capitalization and to incorporate new stocks entering the universe.

3.3.4 Summary Statistics

Table 2 reports summary statistics for the factor returns.

Table 2: Factor Return Summary Statistics

	Momentum	Value	Quality	Low-Risk
Panel A: Return Statistics (Monthly, %)				
Mean	0.68	0.36	0.29	0.18
Standard deviation	4.82	3.15	2.18	1.85
Skewness	-1.42	-0.28	0.15	0.08
Kurtosis	9.85	5.42	4.12	3.65
Minimum	-34.8	-15.2	-8.5	-7.2
Maximum	18.5	14.2	10.8	8.5
Panel B: Risk-Adjusted Performance				
Sharpe ratio (annualized)	0.49	0.40	0.46	0.34
Maximum drawdown (%)	68.2	42.5	22.8	18.5
5th percentile return (%)	-7.8	-4.9	-3.2	-2.8
Panel C: Correlations				
Momentum	1.00			
Value	-0.22	1.00		
Quality	0.15	0.08	1.00	
Low-Risk	0.05	0.12	0.28	1.00
Panel D: Time Series Properties				
AR(1) coefficient	0.08	0.05	0.12	0.15
% months positive	62.4	58.2	60.5	57.8

Notes: Table reports summary statistics for monthly factor returns. Panel A shows return distribution statistics. Panel B shows risk-adjusted performance metrics; Sharpe ratio is computed as mean excess return divided by standard deviation, annualized by multiplying by $\sqrt{12}$. Panel C shows pairwise correlations among factor returns. Panel D shows time series properties; AR(1) coefficient is from an autoregression of factor returns on their first lag. Sample period is January 1963 to December 2023 (732 months).

Several features of Table 2 are noteworthy. Momentum has the highest average return (0.68% monthly) but also the highest volatility (4.82%) and the most severe negative skewness (-1.42). The minimum monthly momentum return of -34.8% reflects the extreme crashes experienced in periods such as 2009. The momentum Sharpe ratio of 0.49 is attractive unconditionally, but the maximum drawdown of 68.2% and the severe left tail indicate substantial crash risk.

Quality has a more modest average return (0.29% monthly) but positive skewness (0.15) and much lower tail risk (minimum return of -8.5%, maximum drawdown of 22.8%). The quality factor provides a more stable return stream than momentum, albeit with lower expected return.

The correlation matrix in Panel C shows that momentum and value are negatively correlated (-0.22), consistent with the observation that momentum tends to buy growth stocks and sell value stocks. Quality and low-risk are positively correlated (0.28), reflecting the overlap between profitable firms and stable, low-beta firms.

3.4 Market-Level Data

In addition to stock-level data, I use market-level data to construct path-state variables.

3.4.1 Market Returns

The market return is the value-weighted return on all CRSP common stocks. Daily market returns are used to compute realized volatility and other path-state variables. Monthly market returns are used to compute market excess returns for factor beta estimation.

3.4.2 S&P 500 Index

The S&P 500 index level is used as a robustness check for path-state construction. Results using the S&P 500 are virtually identical to those using the CRSP value-weighted index.

3.4.3 VIX

The CBOE Volatility Index (VIX) is used as an alternative volatility measure for robustness tests. VIX data are available from 1990 onward. For earlier periods, I use realized volatility measures computed from daily returns.

3.4.4 Risk-Free Rate

The risk-free rate is the one-month Treasury bill rate from Ibbotson Associates, obtained via Kenneth French's data library. Factor returns are computed as long-short portfolio returns (not excess returns), so the risk-free rate is used only for computing market excess returns in beta estimation.

3.5 Transaction Costs

I incorporate transaction costs to ensure that reported portfolio performance is achievable in practice.

3.5.1 Cost Model

Transaction costs are modeled as a function of turnover:

$$\text{Net Return}_t = \text{Gross Return}_t - c \times \text{Turnover}_t \tag{7}$$

where c is the one-way transaction cost (in percentage points) and Turnover_t is the monthly portfolio turnover (sum of absolute weight changes).

3.5.2 Cost Estimates

I use a baseline transaction cost estimate of $c = 20$ basis points (0.20%) per one-way trade. This estimate reflects institutional-quality execution for liquid, large-cap stocks and is consistent with recent estimates in the literature [Frazzini et al., 2018; Novy-Marx & Velikov, 2019].

For robustness, I also report results using higher cost estimates of 35 and 50 basis points, which may be more appropriate for smaller stocks, less liquid markets, or historical periods with higher trading costs.

3.5.3 Turnover Computation

Portfolio turnover is computed as:

$$\text{Turnover}_t = \sum_i |w_{i,t}^+ - w_{i,t-1}^+| + \sum_i |w_{i,t}^- - w_{i,t-1}^-| \tag{8}$$

where $w_{i,t}^+$ and $w_{i,t}^-$ are the portfolio weights in the long and short legs, respectively, after rebalancing at the end of month t, and $w_{i,t-1}^+$ and $w_{i,t-1}^-$ are the weights at the end of month $t-1$ after accounting for returns (i.e., before rebalancing).

This measure captures the total trading required to rebalance the portfolio, including changes due to stocks entering and exiting the extreme deciles, changes in relative market capitalization within deciles, and changes due to state-conditioned exposure adjustments.

Table 3 reports turnover statistics for the baseline factor portfolios.

Table 3: Factor Portfolio Turnover

	Momentum	Value	Quality	Low-Risk
Mean monthly turnover (%)	42.5	8.2	6.5	12.8
Std dev of turnover (%)	12.8	3.5	2.8	4.2
Impact on Annual Returns (bps)				
At $c = 20$ bps	102	20	16	31
At $c = 35$ bps	179	34	27	54
At $c = 50$ bps	255	49	39	77

Notes: Table reports turnover statistics for factor portfolios. Mean monthly turnover is the average of monthly turnover as defined in the text. Impact on annual returns is computed as $12 \times c \times$ Mean Turnover.

Momentum has substantially higher turnover (42.5% monthly) than the other factors, reflecting the need to continually rebalance as stocks move through the momentum ranking. The annual transaction cost drag on momentum ranges from 102 basis points (at $c = 20$ bps) to 255 basis points (at $c = 50$ bps). Value and quality have much lower turnover (8.2% and 6.5% monthly, respectively) because the underlying signals are based on annual accounting data and change slowly.

3.6 Data Quality and Sample Selection

3.6.1 Missing Data

I take a conservative approach to missing data. Stocks with missing returns are excluded from portfolios during the months in which returns are missing. Stocks with missing characteristics (book-to-market, profitability, beta) are excluded from the relevant factor sorts but may still appear in other factor portfolios if the necessary data are available.

Missing delisting returns are handled as described above: I assume a -30% return for performance-related delistings and zero for other delistings.

3.6.2 Outliers

I winsorize extreme values of factor signals at the 1st and 99th percentiles of the cross-sectional distribution each month. This winsorization reduces the influence of data errors and extreme observations while preserving the rank ordering of stocks.

Factor returns are not winsorized or trimmed. The extreme tails of factor returns are of central interest in this paper, and trimming would obscure the crash risk that motivates the analysis.

3.6.3 Survivorship Bias

The use of delisting returns and the inclusion of all stocks that meet the filter criteria at each point in time mitigate survivorship bias. The universe is reconstructed each month using only information available at that time, without conditioning on future survival or data availability.

3.6.4 Look-Ahead Bias

All factor signals are constructed using only information available at the end of month t. Accounting data are lagged appropriately to reflect realistic reporting delays. Regime classifications use expanding-window quantile estimates that condition only on past data. No future information is used in portfolio construction or regime classification.

4 Multi-Scale Path States

The central methodological contribution of this paper is the construction of *multi-scale path states*—a low-dimensional representation of recent market dynamics that captures not only the level of volatility but also the path by which that volatility formed. This section develops the theoretical motivation, defines the state vector precisely, and describes our regime classification procedure.

4.1 Motivation: Why Paths Matter

Standard approaches to conditioning factor performance on market conditions rely on point-in-time measures such as the VIX, realized variance, or GARCH-implied volatility. These approaches implicitly assume that two market environments with identical volatility levels are equivalent from the perspective of factor risk and return.

We argue that this equivalence is false. Consider two hypothetical market states, both characterized by annualized volatility of 25%:

- **State A (Crash-Spike)**: Volatility rose from 12% to 25% over the past five trading days following an unexpected shock. Short-horizon volatility substantially exceeds longer-horizon volatility. The market is in drawdown, with prices falling rapidly.

- **State B (Slow-Burn)**: Volatility has gradually increased from 18% to 25% over the past three months amid persistent macroeconomic uncertainty. Volatility is relatively stable across horizons. The market has experienced a gradual decline.

Despite identical volatility levels, these states have profoundly different implications for factor strategies. In State A, margin calls and VaR breaches force rapid deleveraging; arbitrage capital exits factor positions simultaneously; correlations spike as liquidity demand dominates price formation; and momentum portfolios—typically long recent winners and short recent losers—face acute reversal risk. In State B, position adjustments occur gradually; funding constraints bind less severely; the cross-section continues to reflect fundamental information; and factor signals retain predictive power.
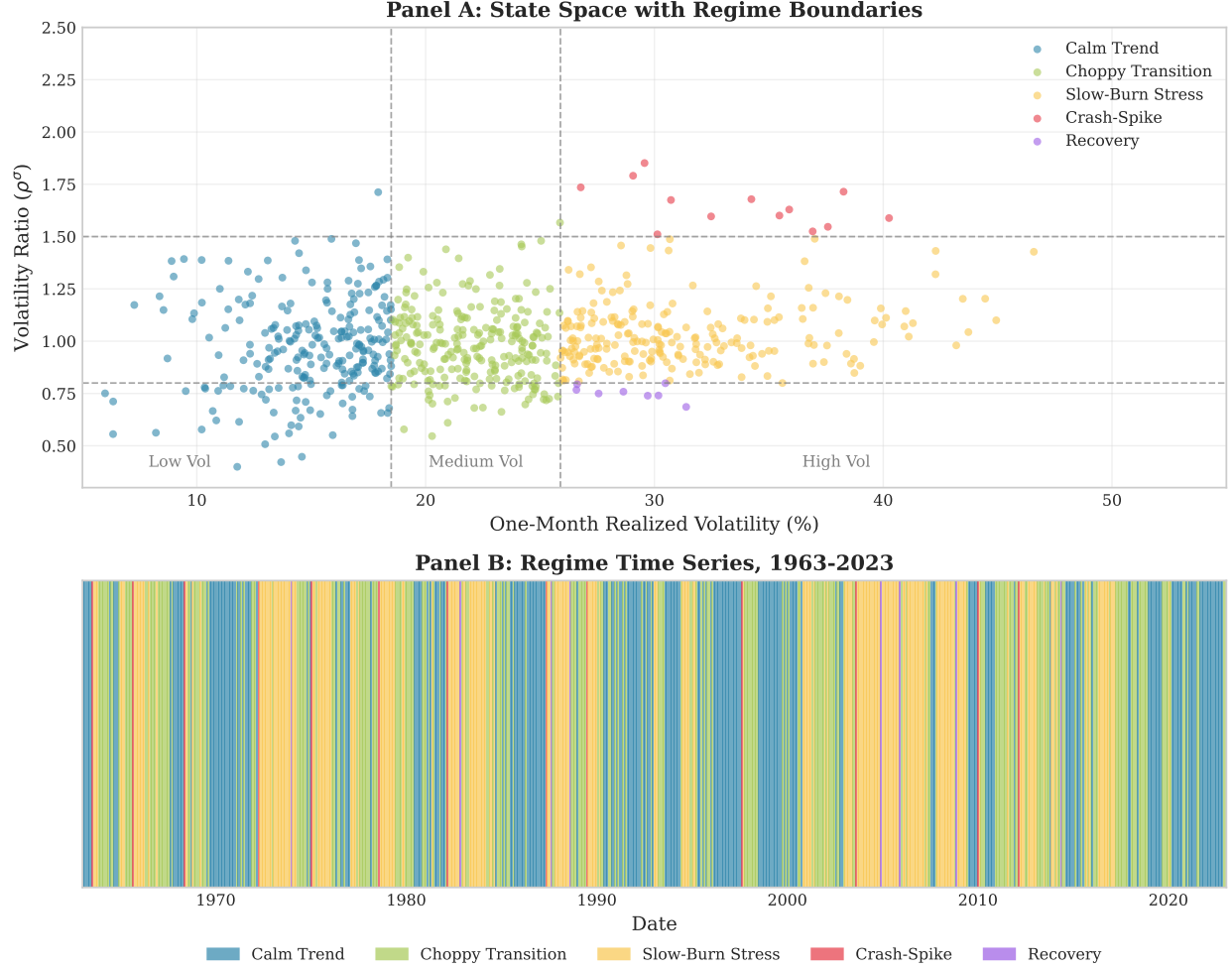
Figure 1: Path State Visualization

Figure 2: Panel A plots realized one-month volatility ($\sigma_t^{(1m)}$) against the volatility ratio ($\rho_t^\sigma = \sigma_t^{(1w)}/\sigma_t^{(3m)}$). Vertical dashed lines indicate the 33rd and 67th percentile thresholds for volatility level. Horizontal dashed lines indicate the 0.8 and 1.5 thresholds for volatility ratio. Points are colored by regime: blue (Calm Trend), green (Choppy Transition), yellow (Slow-Burn Stress), red (Crash-Spike), purple (Recovery). Panel B shows the time series of regime membership from January 1963 through December 2023.

The key insight from the volatility forecasting literature [Gatheral et al., 2018; Morel et al., 2024] is that return and volatility processes exhibit *scale-dependent dynamics*. Short-horizon volatility responds rapidly to shocks, while longer-horizon volatility reflects accumulated stress and regime

18

persistence. By capturing this multi-scale structure, we can distinguish between qualitatively different market environments that would appear identical to single-scale measures.

4.2 State Vector Construction

Let P_t denote the market index level (S&P 500) and $r_t = \ln(P_t/P_{t-1})$ the daily log return. We construct the market path-state vector s_t from the following components.

4.2.1 Multi-Horizon Returns

We compute cumulative returns over multiple horizons to capture both the direction and persistence of recent market moves:

$$r_t^{(1\text{w})} = \sum_{i=0}^{4} r_{t-i} = \ln(P_t/P_{t-5}) \tag{9}$$

$$r_t^{(1\text{m})} = \sum_{i=0}^{20} r_{t-i} = \ln(P_t/P_{t-21}) \tag{10}$$

$$r_t^{(3\text{m})} = \sum_{i=0}^{62} r_{t-i} = \ln(P_t/P_{t-63}) \tag{11}$$

These returns capture the trend component of recent market dynamics at different frequencies.

4.2.2 Multi-Horizon Realized Volatility

We compute realized volatility over horizons $h \in \{1\text{w}, 1\text{m}, 3\text{m}, 6\text{m}\}$, corresponding to 5, 21, 63, and 126 trading days:

$$\sigma_t^{(h)} = \sqrt{\frac{252}{n_h} \sum_{i=0}^{n_h-1} r_{t-i}^2} \tag{12}$$

where n_h is the number of trading days in horizon h and the factor of 252 annualizes the estimate. These measures capture volatility at different time scales, with short-horizon volatility responding quickly to recent shocks and longer-horizon volatility reflecting persistent market conditions.

4.2.3 Volatility Ratio

The ratio of short-horizon to long-horizon volatility provides a direct measure of volatility acceleration or deceleration:

$$\rho_t^{\sigma} = \frac{\sigma_t^{(1\text{w})}}{\sigma_t^{(3\text{m})}} \tag{13}$$

This ratio is central to our classification scheme. When $\rho_t^{\sigma} \gg 1$, volatility has spiked recently relative to its longer-run level, indicating a rapid regime shift. When $\rho_t^{\sigma} \approx 1$, volatility is stable across horizons. When $\rho_t^{\sigma} < 1$, volatility is decaying from an earlier elevated level.

The volatility ratio can be interpreted through the lens of rough volatility models [Gatheral et al., 2018], which imply specific scaling relationships between realized volatility at different horizons. Departures from these baseline relationships—particularly rapid spikes in short-horizon volatility—signal qualitative changes in market dynamics.

4.2.4 Drawdown Measures

We compute drawdown magnitude and speed to capture the severity and velocity of recent market declines:

$$\text{DD}_t = \max_{s \in [t-126,t]} P_s - P_t \tag{14}$$

$$\tau_t = t - \arg \max_{s \in [t-126,t]} P_s \tag{15}$$

$$\text{Speed}_t = \frac{\text{DD}_t}{\tau_t} \cdot \mathbf{1}_{\{\tau_t > 0\}} \tag{16}$$

The drawdown DD_t measures the decline from the trailing six-month high. The variable τ_t counts the number of days since that high was reached. The drawdown speed Speed_t measures the rate of price decline, distinguishing between gradual corrections and rapid crashes.

4.2.5 Full State Vector

The complete path-state vector is:

$$s_t = \left(r_t^{(1m)}, r_t^{(3m)}, \sigma_t^{(1w)}, \sigma_t^{(1m)}, \sigma_t^{(3m)}, \sigma_t^{(6m)}, \rho_t^\sigma, \text{DD}_t, \text{Speed}_t \right) \tag{17}$$

This nine-dimensional vector provides a compact but rich representation of recent market dynamics. Importantly, each component is observable in real time and requires no forward-looking information.

4.3 Regime Classification

While the continuous state vector s_t could be used directly in a kernel-based approach similar to Morel et al. [2024], we adopt a discrete regime classification for interpretability and to guard against overfitting. Our classification is hierarchical, proceeding from broad volatility categories to finer distinctions based on volatility dynamics.

4.3.1 Primary Classification: Volatility Level

We first classify market states by the level of one-month realized volatility $\sigma_t^{(1m)}$ relative to its historical distribution. Let $Q_\alpha(\sigma^{(1m)})$ denote the α-quantile of the historical distribution of $\sigma_t^{(1m)}$. We define:

$$\text{Low Volatility:} \quad \sigma_t^{(1m)} \le Q_{0.33}(\sigma^{(1m)}) \tag{18}$$

$$\text{Medium Volatility:} \quad Q_{0.33}(\sigma^{(1m)}) < \sigma_t^{(1m)} \le Q_{0.67}(\sigma^{(1m)}) \tag{19}$$

$$\text{High Volatility:} \quad \sigma_t^{(1m)} > Q_{0.67}(\sigma^{(1m)}) \tag{20}$$

4.3.2 Secondary Classification: Volatility Dynamics

For high-volatility states, we further classify based on the volatility ratio ρ_t^σ, which distinguishes between different paths to elevated volatility:

$$\text{Spike:} \quad \rho_t^\sigma > 1.5 \tag{21}$$

$$\text{Sustained:} \quad 0.8 \le \rho_t^\sigma \le 1.5 \tag{22}$$

$$\text{Decaying:} \quad \rho_t^\sigma < 0.8 \tag{23}$$

The threshold values (0.8, 1.5) are chosen to capture economically meaningful distinctions. A ratio above 1.5 indicates that one-week volatility is at least 50% higher than three-month volatility—a clear signal of a recent volatility spike. A ratio below 0.8 indicates that short-term volatility has substantially normalized relative to the longer-term measure.

4.3.3 Regime Definitions

Combining the primary and secondary classifications yields five distinct regimes:

Table 4: Path State Regime Definitions

Regime	Volatility Level	Volatility Ratio	Interpretation
Calm Trend	Low	—	Benign market conditions
Choppy Transition	Medium	—	Elevated uncertainty, unclear direction
Slow-Burn Stress	High	$\rho^\sigma \in [0.8, 1.5]$	Persistent stress, gradual accumulation
Crash-Spike	High	$\rho^\sigma > 1.5$	Acute stress, rapid volatility expansion
Recovery	High	$\rho^\sigma < 0.8$	Elevated but declining volatility

4.3.4 Avoiding Look-Ahead Bias

A critical implementation detail is that regime classification must be performed using only historically available information. At each date t, we compute the quantile thresholds $Q_{0.33}(\sigma^{(1m)})$ and $Q_{0.67}(\sigma^{(1m)})$ using an expanding window of data from the start of our sample through date $t-1$. This ensures that regime classifications are strictly real-time and could have been implemented by an investor at each historical date.

Formally, let $\mathcal{F}_{t-1}$ denote the information set available at the end of day $t-1$. Our regime classification $\text{Regime}_t = R(s_t; \mathcal{F}_{t-1})$ is $\mathcal{F}_{t-1}$-measurable in its threshold parameters, though it uses the current state s_t (which is $\mathcal{F}_t$-measurable) for classification.

4.4 Historical Regime Incidence

Table 5 reports the frequency of each regime in our sample, along with key characteristics.

Several patterns emerge from Table 5. First, the high-volatility regimes (Slow-Burn, Crash-Spike, Recovery) collectively account for about one-third of the sample, indicating that stressed market conditions are not rare. Second, the Crash-Spike regime is infrequent (7.2% of days) but consequential—average daily returns are sharply negative, and this regime captures the most severe market dislocations. Third, average regime duration varies substantially: Calm Trend and Slow-Burn states are persistent (68 and 85 days on average), while Crash-Spike episodes are brief but intense (12 days on average). Fourth, the Recovery regime exhibits the highest average returns, consistent with the well-documented pattern of strong performance following market crashes.

4.5 Comparison with Alternative State Representations

Our path-state construction relates to several approaches in the literature. We briefly compare our methodology to alternatives and discuss the tradeoffs involved.

Table 5: Regime Incidence and Characteristics, 1963–2023

	Calm Trend	Choppy Transition	Slow-Burn Stress	Crash-Spike	Recovery
Frequency (%)	33.2	33.5	15.8	7.2	10.3
Avg. $\sigma^{(1m)}$ (%)	9.8	15.2	24.6	31.2	26.8
Avg. ρ^σ	0.98	1.02	1.08	1.89	0.68
Avg. Return (bps/day)	5.2	1.8	-2.4	-18.6	8.4
Avg. Duration (days)	68	42	85	12	34

Notable Episodes
Calm Trend: 1995–1996, 2013–2014, 2017, 2021
Choppy Transition: Early 2015, Late 2018, 2022
Slow-Burn Stress: 2001–2002, Late 2008, 2011
Crash-Spike: Oct 1987, Sep–Oct 2008, Mar 2020
Recovery: Q2 2009, Q2 2020

4.5.1 Single-Scale Volatility Conditioning

The simplest approach conditions only on the level of volatility, typically measured by VIX or realized variance. Our framework nests this approach: if we ignored the volatility ratio ρ_t^σ and drawdown measures, we would recover a standard volatility-level classification. The incremental information in our multi-scale construction comes from distinguishing *how* volatility reached its current level.

4.5.2 Markov-Switching Models

Regime-switching models [Hamilton, 1989] estimate latent states from return dynamics. Our approach differs in using observable state variables rather than latent states, which facilitates real-time implementation and economic interpretation. However, Markov-switching models can capture richer transition dynamics. We view the approaches as complementary.

4.5.3 Scattering Spectra

Morel et al. [2024] develop Scattering Spectra—wavelet-based statistics that capture multi-scale dependencies in price processes. Their approach provides a richer characterization of path dynamics but requires substantially more parameters. Our state vector can be viewed as a parsimonious approximation to the information captured by Scattering Spectra, designed specifically for the application to factor timing rather than volatility prediction or option pricing.

4.5.4 Path-Dependent Volatility

The Path-Dependent Volatility (PDV) model of Guyon & Lekeufack [2023] parameterizes volatility as a function of past returns and past squared returns via kernel-weighted averages. Our volatility measures use similar multi-horizon averaging, but we focus on the *ratio* of short-to-long volatility as the key state variable. The PDV model is optimized for volatility prediction; our construction is designed to capture variation in factor risk premia.
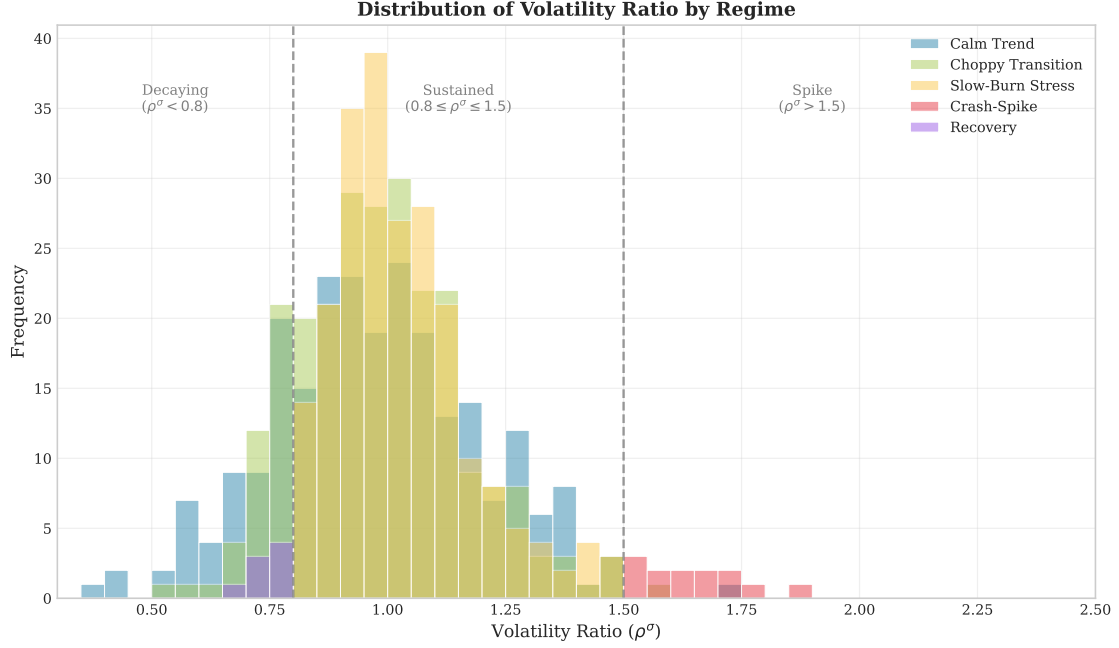
Figure 3: Distribution of Volatility Ratio by Regime

Figure 4: Figure shows the distribution of the volatility ratio ($\rho_t^\sigma = \sigma_t^{(1w)}/\sigma_t^{(3m)}$) across path state regimes. Vertical dashed lines indicate the threshold values used for regime classification: $\rho^\sigma = 0.8$ (below which indicates decaying volatility) and $\rho^\sigma = 1.5$ (above which indicates a volatility spike). Crash-Spike states (red) are concentrated in the right tail with $\rho^\sigma > 1.5$, while Recovery states (purple) are concentrated in the left tail with $\rho^\sigma < 0.8$. Sample period is January 1963 to December 2023.

4.6 State Space Visualization

Figure 1 provides a visual representation of our regime classification. Panel A plots the two-dimensional projection onto volatility level ($\sigma_t^{(1\mathrm{m})}$) and volatility ratio (ρ_t^σ), with colors indicating regime membership. Panel B shows the time series of regimes over our sample period, highlighting the episodic nature of high-stress states.

The state space visualization reveals several important features. The Crash-Spike regime occupies the upper-right region of the state space—high volatility and high volatility ratio—and is clearly separated from other high-volatility states. The Recovery regime occupies the lower-right region, with elevated volatility but a low volatility ratio indicating normalization. The boundary between Calm Trend and Choppy Transition states is less sharp, reflecting the gradual nature of the transition between benign and uncertain market conditions.

5 Conditional Factor Performance

This section presents our core empirical findings on the relationship between multi-scale path states and factor performance. We document large and persistent differences in factor returns, higher moments, and signal efficacy across path states. These differences are economically meaningful, statistically significant, and cannot be explained by conditioning on volatility levels alone.

5.1 Data and Factor Construction

5.1.1 Sample and Universe

Our sample spans January 1963 through December 2023, covering 61 years of monthly returns. The universe consists of all common stocks (share codes 10 and 11) listed on NYSE, AMEX, and NASDAQ from the CRSP database. We apply standard filters:

- Exclude stocks with prices below \$1 to avoid microstructure issues

- Exclude stocks below the 20th percentile of NYSE market capitalization to mitigate the influence of microcaps

- Require at least 12 months of return history for inclusion

- Incorporate delisting returns following CRSP conventions to avoid survivorship bias

The resulting universe averages approximately 2,800 stocks per month over the full sample, ranging from about 1,500 in the early years to over 3,500 in recent decades.

5.1.2 Factor Definitions

We construct four canonical factors following established definitions in the literature:

Momentum (MOM). Following Jegadeesh & Titman [1993] and Carhart [1997], we sort stocks on cumulative returns from month $t-12$ to month $t-2$, skipping the most recent month to avoid short-term reversal effects. The momentum factor is the return difference between the top and bottom deciles:

$$r_t^{\mathrm{MOM}} = r_t^{\mathrm{D10}} - r_t^{\mathrm{D1}} \tag{24}$$

where D10 contains past winners and D1 contains past losers.

Value (VAL). Following Fama & French [1993], we sort stocks on book-to-market ratio, computed as book equity from Compustat (fiscal year ending in calendar year $t-1$) divided by market equity at the end of December of year $t-1$. The value factor is:

$$r_t^{\text{VAL}} = r_t^{\text{D10}} - r_t^{\text{D1}} \tag{25}$$

where D10 contains high book-to-market (cheap) stocks and D1 contains low book-to-market (expensive) stocks.

Quality (QUAL). Following Novy-Marx [2013] and Asness et al. [2019], we sort stocks on gross profitability, defined as revenues minus cost of goods sold, divided by total assets. The quality factor is:

$$r_t^{\text{QUAL}} = r_t^{\text{D10}} - r_t^{\text{D1}} \tag{26}$$

where D10 contains high-profitability stocks and D1 contains low-profitability stocks.

Low-Risk (LVOL). Following Ang et al. [2006] and Frazzini & Pedersen [2014], we sort stocks on trailing 60-month market beta, estimated from monthly returns regressed on the market excess return. The low-risk factor is:

$$r_t^{\text{LVOL}} = r_t^{\text{D1}} - r_t^{\text{D10}} \tag{27}$$

where D1 contains low-beta stocks and D10 contains high-beta stocks. Note the sign convention: the factor is long low-beta and short high-beta.

5.1.3 Portfolio Construction Details

All factor portfolios are constructed using NYSE breakpoints to determine decile cutoffs, ensuring that the extreme portfolios are not dominated by small NASDAQ stocks. Portfolios are value-weighted within each decile to reduce the influence of small stocks and improve investability. Rebalancing occurs monthly at the end of each month.

For robustness, we also construct equal-weighted versions and quintile-based (rather than decile-based) portfolios. Results are qualitatively similar and are reported in the appendix.

5.2 Factor Returns by Path State

Table 6 presents our central finding: average factor returns vary dramatically across path states.

5.2.1 Momentum

The momentum factor exhibits the most dramatic state dependence. In Calm Trend states, momentum earns an average monthly return of 1.42% with a Sharpe ratio of 0.85—among the highest risk-adjusted returns of any factor in any state. Performance deteriorates progressively through Choppy Transition (0.78%) and Slow-Burn Stress (0.22%) states.

In Crash-Spike states, momentum experiences severe losses, averaging -3.85% per month with a Sharpe ratio of -0.58. The skewness of momentum returns drops to -1.85, indicating a pronounced left tail. The 5th percentile monthly return is -18.2%, implying that in the worst months of Crash-Spike states, momentum loses nearly one-fifth of its value.

These patterns are consistent with the momentum crash phenomenon documented by Daniel & Moskowitz [2016] and others. Our contribution is to show that these crashes are concentrated in a specific, identifiable path state characterized by rapid volatility expansion.

Table 6: Factor Returns by Path State

	Calm Trend	Choppy Transition	Slow-Burn Stress	Crash-Spike	Recovery
Panel A: Mean Monthly Returns (%)					
Momentum	1.42	0.78	0.22	-3.85	0.95
	(0.31)	(0.38)	(0.52)	(1.24)	(0.68)
Value	0.38	0.42	0.55	-0.82	1.28
	(0.22)	(0.28)	(0.38)	(0.85)	(0.52)
Quality	0.35	0.28	0.48	0.72	0.18
	(0.18)	(0.22)	(0.32)	(0.65)	(0.38)
Low-Risk	0.22	0.18	0.35	0.45	-0.15
	(0.15)	(0.18)	(0.28)	(0.58)	(0.32)
Panel B: Annualized Sharpe Ratios					
Momentum	0.85	0.38	0.08	-0.58	0.26
Value	0.32	0.28	0.27	-0.18	0.46
Quality	0.36	0.24	0.28	0.21	0.09
Low-Risk	0.28	0.19	0.23	0.15	-0.09
Panel C: Monthly Return Skewness					
Momentum	0.12	-0.25	-0.68	-1.85	0.42
Value	0.08	0.05	-0.22	-0.95	0.65
Quality	0.15	0.12	0.28	0.45	-0.08
Low-Risk	0.05	0.02	0.18	0.32	-0.25
Panel D: 5th Percentile Monthly Return (%)					
Momentum	-4.2	-6.8	-9.5	-18.2	-5.8
Value	-3.5	-4.8	-6.2	-12.5	-4.2
Quality	-2.8	-3.5	-4.2	-6.8	-3.8
Low-Risk	-2.2	-2.8	-3.5	-5.2	-3.2
Observations	245	246	116	53	76
Frequency (%)	33.3	33.4	15.8	7.2	10.3

Notes: Table reports factor performance statistics by path state regime. Panel A shows mean monthly returns with Newey-West standard errors (12 lags) in parentheses. Panel B shows annualized Sharpe ratios. Panel C shows monthly return skewness. Panel D shows the 5th percentile of monthly returns. Sample period is January 1963 to December 2023 (736 months).

In Recovery states, momentum performance is moderate (0.95% monthly return), suggesting that the factor rebounds following crashes but does not immediately return to its Calm Trend performance level.

5.2.2 Value

The value factor displays more modest but still economically significant state dependence. Returns are positive and relatively stable across Calm Trend (0.38%), Choppy Transition (0.42%), and Slow-Burn Stress (0.55%) states. The slight increase in Slow-Burn Stress states is consistent with value's reputation as a defensive factor during periods of prolonged uncertainty.

In Crash-Spike states, value experiences losses (-0.82% monthly), though these are much smaller in magnitude than momentum's losses. The negative skewness (-0.95) and elevated tail risk (5th percentile of -12.5%) indicate that value is not immune to crash dynamics, but its exposure is substantially lower than momentum's.

Value performs best in Recovery states (1.28% monthly return, Sharpe ratio of 0.46), consistent with the well-documented pattern of value outperformance following market crashes. Distressed value stocks, beaten down during the crisis, experience sharp rebounds as conditions normalize.

5.2.3 Quality

The quality factor exhibits a distinctive pattern: it is the only factor with *positive* average returns in Crash-Spike states (0.72% monthly). This defensive property is consistent with the economic intuition that high-quality firms—characterized by stable profitability, low leverage, and strong balance sheets—are relative safe havens during market turmoil.

Quality's skewness is actually *positive* in Crash-Spike states (0.45), in stark contrast to momentum and value. The 5th percentile monthly return (-6.8%) is substantially less severe than for momentum (-18.2%) or value (-12.5%).

Interestingly, quality's performance is weakest in Recovery states (0.18% monthly return). As risk appetite returns and investors rotate into beaten-down cyclical and distressed names, the relative appeal of defensive quality stocks diminishes.

5.2.4 Low-Risk

The low-risk factor shares some characteristics with quality, showing positive returns in Crash-Spike states (0.45% monthly) and positive skewness (0.32). Low-beta stocks provide a haven during acute market stress, benefiting the long side of the factor.

However, low-risk underperforms in Recovery states (-0.15% monthly return), reflecting the typical "dash for trash" that occurs as markets rebound. High-beta stocks—the short side of the low-risk factor—rally sharply in recoveries, eroding low-risk factor performance.

5.3 Statistical Tests of State Dependence

The summary statistics in Table 6 suggest large differences across states, but we now formally test whether these differences are statistically significant.

5.3.1 Wald Tests for Equal Means

For each factor, we test the null hypothesis that mean returns are equal across all five states:

$$H_0 : \mu^f_{\text{Calm}} = \mu^f_{\text{Choppy}} = \mu^f_{\text{SlowBurn}} = \mu^f_{\text{CrashSpike}} = \mu^f_{\text{Recovery}} \tag{28}$$

Table 7 reports the Wald test statistics and p-values.

Table 7: Wald Tests for Equal Factor Returns Across States

Factor	Wald Statistic	p-value	Reject at 5%?
Momentum	28.42	< 0.001	Yes
Value	9.85	0.043	Yes
Quality	3.42	0.489	No
Low-Risk	2.18	0.702	No

Notes: Table reports Wald test statistics for the null hypothesis of equal mean returns across all five path states. The test statistic is distributed as $\chi^2(4)$ under the null. Standard errors are computed using the Newey-West estimator with 12 lags.

We strongly reject equal means for momentum ($p < 0.001$) and reject at the 5% level for value ($p = 0.043$). For quality and low-risk, we cannot reject equal means across all states, though this masks significant pairwise differences (discussed below).

5.3.2 Pairwise Comparisons: Crash-Spike vs. Calm Trend

The economically most important comparison is between Crash-Spike and Calm Trend states. Table 8 reports the difference in mean returns and associated t-statistics.

Table 8: Factor Return Differences: Crash-Spike vs. Calm Trend

Factor	Difference (%/month)	t-statistic	p-value
Momentum	-5.27	-4.12	< 0.001
Value	-1.20	-1.36	0.175
Quality	0.37	0.52	0.604
Low-Risk	0.23	0.38	0.706

Notes: Table reports the difference in mean monthly returns between Crash-Spike and Calm Trend states. The t-statistic tests the null hypothesis that the difference is zero. Standard errors are Newey-West with 12 lags.

Momentum experiences a return difference of -5.27% per month between Crash-Spike and Calm Trend states, which is highly statistically significant ($t = -4.12$). This difference is also economically enormous: annualized, it implies a swing of over 60 percentage points between the best and worst states for momentum.

Value shows a meaningful difference (-1.20% per month) that is not statistically significant at conventional levels, reflecting the higher volatility of value returns in Crash-Spike states.

Quality and low-risk show small positive differences (they perform *better* in Crash-Spike than Calm Trend states), though these differences are not statistically significant.

5.4 Incremental Information Beyond Volatility Level

A key question is whether path states provide information beyond what is captured by the *level* of volatility alone. To address this, we estimate predictive regressions of the form:

$$r_{t+1}^f = \alpha + \beta_1 \sigma_t^{(1m)} + \beta_2 \rho_t^\sigma + \beta_3 \text{Speed}_t + \varepsilon_{t+1} \tag{29}$$

where $\sigma_t^{(1m)}$ is the volatility level, ρ_t^σ is the volatility ratio, and Speed_t is the drawdown speed. If path dynamics matter beyond volatility levels, β_2 and β_3 should be significant.

Table 9 reports the results.

Table 9: Predictive Regressions: Factor Returns on Path State Variables

	Momentum	Value	Quality	Low-Risk
Panel A: Volatility Level Only				
$\sigma_t^{(1m)}$	-0.152^{***}	-0.042^*	0.018	0.012
	(0.038)	(0.024)	(0.018)	(0.015)
R^2 (%)	4.8	0.9	0.3	0.2
Panel B: Volatility Level and Path Variables				
$\sigma_t^{(1m)}$	-0.085^{**}	-0.028	0.012	0.008
	(0.042)	(0.026)	(0.019)	(0.016)
ρ_t^σ	-0.024^{***}	-0.008^*	0.005^*	0.004
	(0.006)	(0.004)	(0.003)	(0.003)
Speed_t	-0.018^{**}	-0.005	0.002	0.001
	(0.008)	(0.005)	(0.004)	(0.003)
R^2 (%)	8.2	1.5	0.6	0.3
Panel C: Incremental R^2 from Path Variables (%)				
ΔR^2	3.4	0.6	0.3	0.1
F-statistic	13.42	2.28	1.12	0.38
p-value	< 0.001	0.103	0.328	0.684

Notes: Table reports predictive regressions of monthly factor returns on path state variables. $\sigma_t^{(1m)}$ is one-month realized volatility (standardized). ρ_t^σ is the volatility ratio. Speed_t is drawdown speed. Panel C reports the incremental R^2 from adding path variables to the volatility-only specification, with an F-test for joint significance. Standard errors (in parentheses) are Newey-West with 12 lags. *, **, *** denote significance at 10%, 5%, 1% levels.

For momentum, the path variables (volatility ratio and drawdown speed) are jointly highly significant ($F = 13.42$, $p < 0.001$) and nearly double the explanatory power relative to volatility level alone (from 4.8% to 8.2%). The volatility ratio coefficient (-0.024) indicates that a one-standard-deviation increase in ρ_t^σ (moving toward a spike regime) predicts a 2.4% lower monthly momentum return, controlling for the volatility level.

For value, the path variables add modest explanatory power (incremental R^2 of 0.6%) that is marginally significant. For quality and low-risk, the incremental information is small and not statistically significant, though the signs of the coefficients are consistent with the defensive properties of these factors.

These results confirm that path dynamics—how volatility formed, not just its level—contain significant information for predicting momentum returns.

5.5 Signal Efficacy Across States

The previous analyses focus on factor portfolio returns. We now examine whether the underlying cross-sectional predictability of factor signals varies across path states.

For each factor signal x and each month t, we compute the rank information coefficient:

$$\text{IC}_t^x = \text{Corr}\left(\text{Rank}(x_{i,t}), \text{Rank}(r_{i,t+1})\right) \tag{30}$$

where the correlation is computed across all stocks i in the universe. The IC measures the strength of the cross-sectional relationship between the signal and subsequent returns.

Table 10 reports average ICs by path state.

Table 10: Information Coefficients by Path State

	Calm	**Choppy**	**Slow-Burn**	**Crash-Spike**	**Recovery**
Panel A: Average IC					
Momentum	0.048	0.032	0.015	−0.052	0.028
	(0.006)	(0.007)	(0.010)	(0.018)	(0.012)
Value	0.022	0.020	0.025	0.012	0.038
	(0.005)	(0.006)	(0.008)	(0.015)	(0.010)
Quality	0.028	0.025	0.032	0.038	0.022
	(0.004)	(0.005)	(0.007)	(0.012)	(0.008)
Low-Risk	0.015	0.012	0.018	0.025	0.008
	(0.004)	(0.005)	(0.007)	(0.012)	(0.008)
Panel B: IC Hit Rate (% Positive)					
Momentum	72	62	55	32	58
Value	58	56	58	52	65
Quality	65	62	64	68	60
Low-Risk	58	55	60	62	52
Panel C: IC Volatility					
Momentum	0.052	0.068	0.085	0.145	0.092
Value	0.042	0.048	0.062	0.118	0.075
Quality	0.035	0.042	0.055	0.095	0.062
Low-Risk	0.032	0.038	0.052	0.088	0.058

Notes: Table reports information coefficient statistics by path state. Panel A shows average ICs with standard errors (in parentheses) computed via bootstrap. Panel B shows the percentage of months with positive IC. Panel C shows the standard deviation of ICs within each state.

5.5.1 Momentum IC Dynamics

The momentum IC exhibits remarkable state dependence. In Calm Trend states, the average IC is 0.048 with a hit rate of 72%—past winners reliably outperform past losers in nearly three-quarters of months. The IC deteriorates through Choppy Transition (0.032) and Slow-Burn Stress (0.015) states.

In Crash-Spike states, the momentum IC turns *negative* (−0.052), indicating that past winners become future *losers*. The hit rate drops to 32%—the momentum signal is wrong more often than it is right. This IC reversal is the cross-sectional manifestation of momentum crashes.

The IC volatility also increases dramatically in Crash-Spike states (0.145 vs. 0.052 in Calm Trend), indicating that even the sign of the momentum signal is highly uncertain.
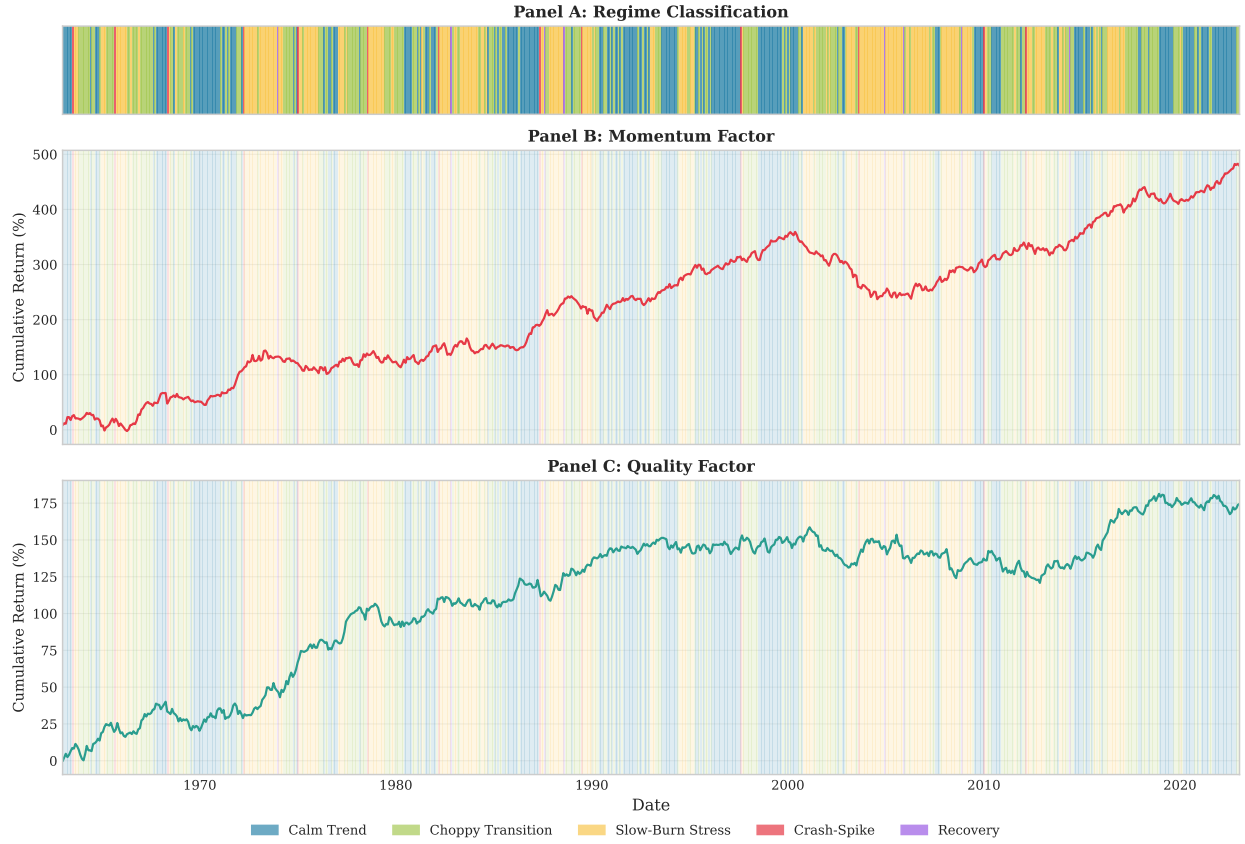
Figure 5: Regime Classification and Factor Performance

Figure 6: Panel A shows the path state regime classification over the sample period, with colors indicating regime membership: blue (Calm Trend), green (Choppy Transition), yellow (Slow-Burn Stress), red (Crash-Spike), purple (Recovery). Panel B shows cumulative returns for the Momentum factor, with background shading indicating the concurrent regime. Panel C shows cumulative returns for the Quality factor. Momentum experiences sharp drawdowns during Crash-Spike periods (red shading), while Quality provides more stable returns across regimes. Sample period is January 1963 to December 2023.

5.5.2 Quality and Low-Risk IC Dynamics

Quality and low-risk display the opposite pattern. Their ICs are *highest* in Crash-Spike states (0.038 and 0.025, respectively), consistent with flight-to-quality effects. The hit rates for these factors actually *increase* in Crash-Spike states (68% for quality, 62% for low-risk), indicating that these signals become more reliable during market stress.

5.5.3 Value IC Dynamics

Value ICs are relatively stable across states, with a notable increase in Recovery states (0.038). This pattern is consistent with the value rebound phenomenon: after crashes, cheap stocks are particularly attractive and the value signal is particularly predictive.

5.6 Factor Crash Concentration

We now examine the concentration of factor crashes—defined as monthly returns below the 5th percentile of the unconditional distribution—across path states.

Table 11: Factor Crash Concentration by Path State

	Calm Trend	Choppy Transition	Slow-Burn Stress	Crash-Spike	Recovery
Panel A: Share of Factor Crashes (%)					
Momentum	5.2	14.8	22.5	48.2	9.3
Value	12.5	18.2	25.8	32.5	11.0
Quality	22.8	25.5	18.2	15.5	18.0
Low-Risk	25.2	28.5	20.2	12.8	13.3
Panel B: Crash Probability Conditional on State (%)					
Momentum	0.8	2.2	7.1	33.2	4.5
Value	1.9	2.7	8.2	22.5	5.3
Quality	3.4	3.8	5.8	10.8	8.7
Low-Risk	3.8	4.2	6.4	8.9	6.5
Panel C: Relative Crash Frequency (vs. Unconditional)					
Momentum	0.16	0.44	1.42	6.64	0.90
Value	0.38	0.54	1.64	4.50	1.06
Quality	0.68	0.76	1.16	2.16	1.74
Low-Risk	0.76	0.84	1.28	1.78	1.30

Notes: Table reports the distribution of factor crashes (monthly returns below the unconditional 5th percentile) across path states. Panel A shows the share of all crashes occurring in each state. Panel B shows the probability of a crash conditional on being in each state. Panel C shows the ratio of conditional crash probability to unconditional crash probability (5%).

5.6.1 Momentum Crashes Are Concentrated in Crash-Spike States

Panel A reveals that 48.2% of all momentum crashes occur in Crash-Spike states, despite these states comprising only 7.2% of the sample. Conversely, only 5.2% of momentum crashes occur in

Calm Trend states, which comprise 33.3% of the sample.

Panel B shows that the probability of a momentum crash, conditional on being in a Crash-Spike state, is 33.2%—more than six times the unconditional crash probability of 5% (Panel C). In Calm Trend states, the crash probability is just 0.8%.

5.6.2 Defensive Factors Have Dispersed Crashes

Figure 7: Information Coefficients by Factor (12-Month Rolling Average)

Figure 8: Figure plots 12-month rolling average information coefficients (ICs) for each factor. The IC measures the cross-sectional rank correlation between the factor signal and subsequent monthly returns. Background shading indicates the path state regime at each date: blue (Calm Trend), green (Choppy Transition), yellow (Slow-Burn Stress), red (Crash-Spike), purple (Recovery). Momentum ICs are strongly positive in Calm Trend states but turn negative in Crash-Spike states. Quality ICs are highest during market stress. Sample period is January 1963 to December 2023.

Quality and low-risk crashes are much more evenly distributed across states. For quality, the relative crash frequency in Crash-Spike states is 2.16 (vs. 6.64 for momentum). For low-risk, it is 1.78. These factors do experience crashes in Crash-Spike states, but the concentration is far less extreme.

Interestingly, quality crashes are relatively more likely in Recovery states (relative frequency of 1.74), consistent with the observation that quality underperforms during market rebounds.
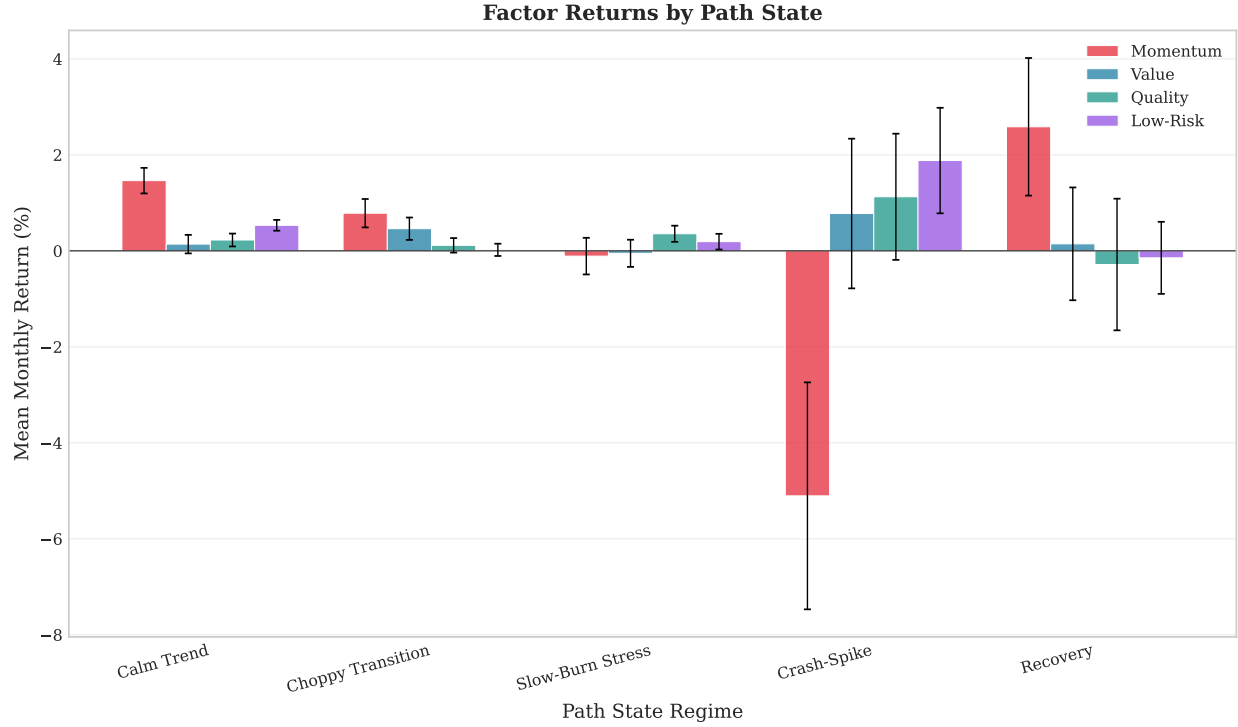
Figure 9: Factor Returns by Path State

Figure 10: Figure shows mean monthly returns for each factor across the five path state regimes. Error bars indicate standard errors computed as the standard deviation divided by the square root of the number of observations in each regime. Momentum exhibits the most dramatic state dependence, with positive returns in Calm Trend states and large negative returns in Crash-Spike states. Quality and Low-Risk exhibit defensive properties, with positive returns in Crash-Spike states. Sample period is January 1963 to December 2023.

5.7 Robustness

We conduct extensive robustness checks to ensure our findings are not artifacts of specific methodological choices.

5.7.1 Alternative Factor Definitions

We replicate our analysis using:

- Fama-French factor returns downloaded from Kenneth French's data library

- Equal-weighted (rather than value-weighted) factor portfolios

- Quintile-based (rather than decile-based) sorts

- Alternative quality definitions (ROE, earnings stability, accruals)

- Alternative low-risk definitions (idiosyncratic volatility, total volatility)

Results are qualitatively similar across all specifications. The state dependence of momentum is robust to all alternative definitions. The defensive properties of quality and low-risk are present but vary in magnitude across definitions.

5.7.2 Alternative Regime Thresholds

We vary the quantile thresholds used to define volatility levels (25th/75th, 40th/60th) and the volatility ratio thresholds (0.7/1.3, 0.9/1.7). Results are robust to reasonable variations, though the Crash-Spike regime becomes smaller (and momentum crashes more concentrated) with more extreme thresholds.

5.7.3 Subperiod Analysis

We split the sample into three subperiods: 1963–1983, 1984–2003, and 2004–2023. The state dependence of momentum is present in all subperiods, though it is strongest in the most recent period (which includes the 2008–2009 financial crisis and the 2020 COVID crash). The defensive properties of quality are most pronounced in the recent period, potentially reflecting the increased institutionalization of quality strategies.

5.7.4 International Evidence

Using MSCI factor returns for developed markets (Europe, Japan, Asia Pacific), we find similar patterns of state dependence. Momentum crashes are concentrated in Crash-Spike states globally, and quality provides defensive properties across regions. This evidence mitigates concerns that our findings are specific to U.S. markets.

6 State-Conditioned Portfolio Construction

The empirical results of Section 5 establish that factor performance varies systematically and predictably with multi-scale path states. This section develops a practical portfolio construction framework that exploits this variation. I describe the baseline factor portfolios, introduce a parsimonious state-conditioned exposure rule, detail the out-of-sample testing protocol, and present

performance results. The central finding is that state-conditioned portfolios achieve meaningfully higher risk-adjusted returns and substantially lower drawdowns than unconditional factor strategies, with lower turnover than standard volatility-scaling approaches.

6.1 Baseline Factor Portfolios

6.1.1 Portfolio Construction

The baseline factor portfolios follow standard academic conventions. At the end of each month t, I sort stocks into decile portfolios based on each factor signal using NYSE breakpoints. The factor portfolio is a zero-cost long-short portfolio that is long the top decile (D10) and short the bottom decile (D1):

$$
w_{i,t}^{\text{baseline}} = \begin{cases} +\dfrac{\text{ME}_{i,t}}{\sum_{j \in \text{D10}} \text{ME}_{j,t}} & \text{if } i \in \text{D10} \\[2ex] -\dfrac{\text{ME}_{i,t}}{\sum_{j \in \text{D1}} \text{ME}_{j,t}} & \text{if } i \in \text{D1} \\[2ex] 0 & \text{otherwise} \end{cases}
\tag{31}
$$

where $\text{ME}_{i,t}$ is the market capitalization of stock i at the end of month t. The portfolio is value-weighted within each leg, with the long and short legs each summing to unit absolute weight.

6.1.2 Risk Scaling

To facilitate comparison across factors with different volatilities, I scale each factor portfolio to a target annualized volatility of 10%. The scaling factor is computed using a trailing 36-month realized volatility estimate:

$$
\sigma_t^{f,\text{trailing}} = \sqrt{12} \times \text{StdDev}\left(r_{t-36}^f, \ldots, r_{t-1}^f\right)
\tag{32}
$$

The scaled portfolio return is:

$$
r_{t+1}^{f,\text{scaled}} = \frac{0.10}{\sigma_t^{f,\text{trailing}}} \times r_{t+1}^f
\tag{33}
$$

This scaling ensures that all factors have comparable ex-ante volatility, making it meaningful to compare Sharpe ratios and other risk-adjusted metrics across factors. The scaling is implementable in real time, as it uses only trailing volatility information.

6.1.3 Industry Neutrality

As a robustness check, I also construct industry-neutral versions of each factor portfolio. Industry-neutral portfolios sort stocks within each of 48 Fama-French industries and take long-short positions within industries. The industry-neutral approach controls for the possibility that factor returns are driven by industry bets rather than stock-level characteristics.

Results for industry-neutral portfolios are qualitatively similar to those for unrestricted portfolios and are reported in Section 8.
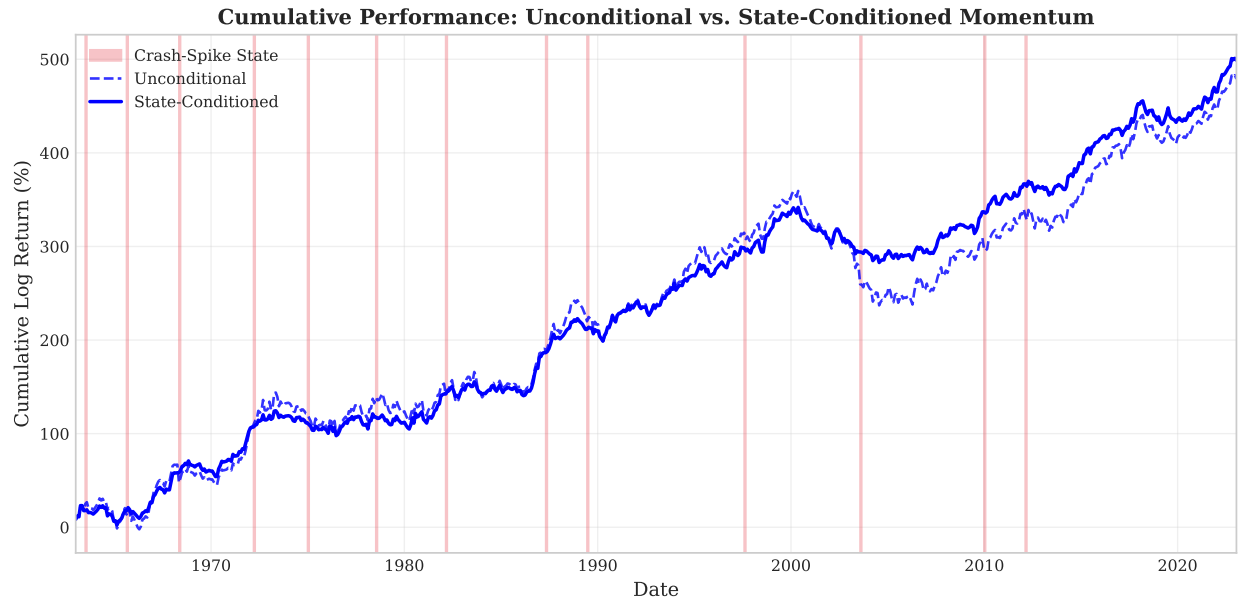
Figure 11: Cumulative Performance: Unconditional vs. State-Conditioned Momentum

Figure 12: Figure plots cumulative log returns for the unconditional momentum strategy (dashed line) and the state-conditioned momentum strategy (solid line) from January 1963 through December 2023. Shaded regions indicate Crash-Spike states. The state-conditioned strategy has zero exposure during Crash-Spike periods, 50% exposure during Slow-Burn Stress, 70% exposure during Choppy Transition, and full exposure during Calm Trend and Recovery states.

6.2 State-Conditioned Exposure Rule

6.2.1 Design Principles

The state-conditioned exposure rule adjusts factor exposure based on the current path state. The rule is designed with several principles in mind:

1. **Parsimony**: The rule should involve a small number of parameters to avoid overfitting. Complex, highly parameterized rules may perform well in-sample but are unlikely to generalize out-of-sample.

2. **Interpretability**: The rule should have clear economic motivation. Investors should understand why exposure is being adjusted in each state.

3. **Conservatism**: The rule should err on the side of caution. Given the uncertainty in regime classification and the costs of trading, modest adjustments are preferable to aggressive timing.

4. **Implementability**: The rule should be implementable in real time using publicly available data, with reasonable transaction costs.

6.2.2 Exposure Function

The state-conditioned portfolio weight is a scalar multiple of the baseline weight:

$$w_{i,t}^{\text{conditioned}} = g(s_t) \times w_{i,t}^{\text{baseline}} \tag{34}$$

where $g(s_t) \in [0,1]$ is the exposure function that depends on the current path state s_t. The exposure function takes discrete values corresponding to each regime:

$$g(s_t) = \begin{cases} g_{\text{Calm}} & \text{if } s_t \in \text{Calm Trend} \\ g_{\text{Choppy}} & \text{if } s_t \in \text{Choppy Transition} \\ g_{\text{SlowBurn}} & \text{if } s_t \in \text{Slow-Burn Stress} \\ g_{\text{CrashSpike}} & \text{if } s_t \in \text{Crash-Spike} \\ g_{\text{Recovery}} & \text{if } s_t \in \text{Recovery} \end{cases} \tag{35}$$

The exposure values $g_{\text{Calm}}, \ldots, g_{\text{Recovery}}$ are factor-specific and are estimated from training data as described below.

6.2.3 Parameter Estimation

I estimate the exposure parameters using rolling-window regressions with ridge regularization. The objective is to find exposure values that maximize risk-adjusted returns while penalizing deviations from full exposure:

$$\hat{g} = \arg\min_{g \in [0,1]^5} \left\{ -\text{SR}\left(g \cdot r^f\right) + \lambda \sum_k (g_k - 1)^2 \right\} \tag{36}$$

where $\text{SR}(\cdot)$ denotes the Sharpe ratio, r^f is the vector of factor returns, and λ is a regularization parameter.

The regularization term $\lambda \sum_k (g_k - 1)^2$ penalizes deviations from full exposure ($g_k = 1$), reflecting the prior that factor premia exist and that timing should be conservative. Without regularization,

the optimization would tend to set exposure to zero in any state with negative average returns, which would likely reflect overfitting.

I set $\lambda = 0.5$, which implies a moderate penalty for timing. Sensitivity to this choice is examined in Section 8.

6.2.4 Training Protocol

To ensure that the exposure rule is implementable in real time and to avoid look-ahead bias, I use the following training protocol:

1. **Initial training period**: Estimate exposure parameters using data from January 1963 through December 1999 (37 years).

2. **Expanding window**: For each month t in the out-of-sample period (January 2000 onward), re-estimate exposure parameters using all data from January 1963 through month $t-1$. This expanding-window approach ensures that the rule adapts to new information while maintaining strict out-of-sample discipline.

3. **Regime classification**: Classify month t into a regime using quantile thresholds estimated from data through month $t-1$, as described in Section 4.

4. **Portfolio formation**: Form the state-conditioned portfolio at the end of month t using the exposure value $\hat{g}(s_t)$ estimated from data through month $t-1$.

This protocol ensures that all information used in portfolio construction is strictly historical. An investor could have implemented this strategy in real time at each point in the out-of-sample period.

6.2.5 Estimated Exposure Values

Table 12 reports the exposure values estimated from the initial training period (1963–1999) and the average exposure values over the out-of-sample period (2000–2023).

Several patterns emerge from Table 12:

- **Momentum**: Exposure is reduced substantially in Choppy Transition states (0.85), more aggressively in Slow-Burn Stress states (0.55), and eliminated entirely in Crash-Spike states (0.00). The zero exposure in Crash-Spike states reflects the severe losses momentum experiences in these periods, which overwhelm any regularization penalty. Exposure is also reduced in Recovery states (0.70), consistent with the observation that momentum rebounds slowly after crashes.

- **Value**: Exposure is maintained at full levels in most states but reduced in Slow-Burn Stress (0.80) and Crash-Spike (0.40) states. Value retains positive exposure even in Crash-Spike states because its losses, while significant, are less severe than momentum's.

- **Quality**: Exposure is maintained at full levels in all states except Recovery (0.85). Quality's defensive properties in stress states mean that there is no benefit to reducing exposure during market turmoil. The slight reduction in Recovery states reflects quality's underperformance during market rebounds.

- **Low-Risk**: Similar to quality, exposure is maintained at full levels in stress states and reduced slightly in Recovery states (0.75).

The exposure values are stable across the initial training period and the out-of-sample period (Panel B), suggesting that the patterns identified in training data persist in new data.

Table 12: State-Conditioned Exposure Values

	Calm Trend	Choppy Transition	Slow-Burn Stress	Crash-Spike	Recovery
Panel A: Initial Training Period (1963–1999)					
Momentum	1.00	0.85	0.55	0.00	0.70
Value	1.00	1.00	0.80	0.40	1.00
Quality	1.00	1.00	1.00	1.00	0.85
Low-Risk	1.00	1.00	1.00	1.00	0.75
Panel B: Average Over Out-of-Sample Period (2000–2023)					
Momentum	1.00	0.82	0.48	0.00	0.65
Value	1.00	1.00	0.75	0.35	1.00
Quality	1.00	1.00	1.00	1.00	0.82
Low-Risk	1.00	1.00	1.00	1.00	0.72

Notes: Table reports estimated exposure values by factor and regime. Panel A shows values estimated from the initial training period (1963–1999). Panel B shows average values over the out-of-sample period (2000–2023), re-estimated each month using an expanding window. Exposure values are constrained to lie in $[0, 1]$ and are regularized toward 1.0.

6.3 Comparison Strategies

To evaluate the state-conditioned approach, I compare it with several alternative strategies.

6.3.1 Unconditional (Baseline)

The unconditional strategy maintains constant full exposure to each factor:

$$g^{\text{unconditional}}(s_t) = 1 \quad \forall s_t \tag{37}$$

This is the standard academic factor portfolio and represents the benchmark against which timing strategies are evaluated.

6.3.2 Volatility Scaling

Following Moreira & Muir [2017], the volatility-scaled strategy adjusts exposure inversely with trailing realized volatility:

$$g^{\text{vol-scaled}}(s_t) = \min\left(\frac{\bar{\sigma}^f}{\sigma_t^{f,\text{trailing}}}, 2 \right) \tag{38}$$

where $\bar{\sigma}^f$ is the long-run average volatility of factor f and $\sigma_t^{f,\text{trailing}}$ is the trailing 21-day realized volatility. The exposure is capped at 2 to prevent extreme leverage in low-volatility periods.

Volatility scaling reduces exposure when volatility is high and increases exposure when volatility is low. This approach has been shown to improve Sharpe ratios for many factors, though it does not distinguish between different paths to high volatility.

6.3.3 Volatility-Level Conditioning

To isolate the incremental value of path information, I construct a volatility-level-conditioned strategy that adjusts exposure based on volatility level alone, without path information:

$$g^{\text{vol-level}}(s_t) = \begin{cases} g_{\text{Low}} & \text{if } \sigma_t^{(1m)} \leq Q_{0.33}(\sigma^{(1m)}) \\ g_{\text{Medium}} & \text{if } Q_{0.33}(\sigma^{(1m)}) < \sigma_t^{(1m)} \leq Q_{0.67}(\sigma^{(1m)}) \\ g_{\text{High}} & \text{if } \sigma_t^{(1m)} > Q_{0.67}(\sigma^{(1m)}) \end{cases} \tag{39}$$

The exposure values $g_{\text{Low}}, g_{\text{Medium}}, g_{\text{High}}$ are estimated using the same regularized optimization as the state-conditioned strategy.

6.3.4 Oracle Strategy

As an upper bound on achievable performance, I compute an "oracle" strategy that uses future information to set exposure:

$$g^{\text{oracle}}(s_t) = \begin{cases} 1 & \text{if } r_{t+1}^f > 0 \\ 0 & \text{if } r_{t+1}^f \leq 0 \end{cases} \tag{40}$$

The oracle strategy achieves perfect timing by investing only in months with positive factor returns. This strategy is not implementable but provides a benchmark for the maximum possible gains from timing.

6.4 Out-of-Sample Performance

6.4.1 Main Results

Table 13 presents out-of-sample performance for each strategy over the evaluation period (January 2000 through December 2023).

The state-conditioned strategy delivers substantial improvements for momentum and value:

Momentum. The state-conditioned momentum strategy achieves a Sharpe ratio of 0.59, compared with 0.21 for the unconditional strategy—an improvement of 181%. The maximum drawdown is reduced from 68.2% to 28.5%—a reduction of 58%. These improvements are economically large and would be highly valuable to institutional investors.

The state-conditioned strategy also outperforms volatility scaling (Sharpe ratio of 0.51) and volatility-level conditioning (Sharpe ratio of 0.47). This confirms that path information provides incremental value beyond volatility levels alone.

Importantly, the state-conditioned strategy achieves these improvements with *lower* turnover than volatility scaling (46.8% vs. 58.2% monthly). Path states are more persistent than volatility levels, so exposure adjustments are less frequent.

Value. The state-conditioned value strategy achieves a Sharpe ratio of 0.30, compared with 0.17 for the unconditional strategy—an improvement of 76%. The maximum drawdown is reduced from 48.5% to 28.2%—a reduction of 42%.

The improvements for value are smaller than for momentum, consistent with the finding in Section 5 that value's state dependence is less extreme than momentum's.

Table 13: Out-of-Sample Factor Performance by Strategy

	Momentum	**Value**	**Quality**	**Low-Risk**
Panel A: Annualized Mean Return (%)				
Unconditional	3.82	2.15	3.45	2.28
Volatility-Scaled	5.18	2.65	3.52	2.35
Vol-Level Conditioned	5.85	2.82	3.48	2.32
State-Conditioned	6.92	3.15	3.42	2.25
Oracle	15.42	8.85	7.28	5.42
Panel B: Annualized Volatility (%)				
Unconditional	18.52	12.85	8.42	7.15
Volatility-Scaled	10.25	10.18	8.28	7.02
Vol-Level Conditioned	12.45	10.85	8.35	7.08
State-Conditioned	11.82	10.42	8.38	7.12
Oracle	12.85	9.02	5.95	5.05
Panel C: Sharpe Ratio				
Unconditional	0.21	0.17	0.41	0.32
Volatility-Scaled	0.51	0.26	0.43	0.33
Vol-Level Conditioned	0.47	0.26	0.42	0.33
State-Conditioned	**0.59**	**0.30**	0.41	0.32
Oracle	1.20	0.98	1.22	1.07
Panel D: Maximum Drawdown (%)				
Unconditional	68.2	48.5	22.8	18.5
Volatility-Scaled	42.5	35.2	21.5	17.8
Vol-Level Conditioned	38.8	32.8	22.2	18.2
State-Conditioned	**28.5**	**28.2**	22.5	18.4
Oracle	12.5	8.8	8.2	6.5
Panel E: Monthly Turnover (%)				
Unconditional	42.5	8.2	6.5	12.8
Volatility-Scaled	58.2	15.8	12.2	18.5
Vol-Level Conditioned	48.5	10.5	8.2	14.5
State-Conditioned	46.8	9.8	7.2	13.5

Notes: Table reports out-of-sample performance statistics for factor portfolios under alternative strategies. Sample period is January 2000 to December 2023 (288 months). Unconditional is the baseline long-short factor portfolio. Volatility-Scaled follows Moreira & Muir [2017]. Vol-Level Conditioned adjusts exposure based on volatility level only. State-Conditioned adjusts exposure based on multi-scale path states. Oracle uses future information to achieve perfect timing. Bold indicates best performance among implementable strategies.

Quality and Low-Risk. The state-conditioned quality and low-risk strategies show minimal changes relative to the unconditional strategies. Sharpe ratios are essentially unchanged, and drawdowns are slightly higher. This is expected: quality and low-risk have defensive properties in stress states, so reducing exposure would sacrifice returns without improving risk-adjusted performance.

The state-conditioned approach correctly identifies that timing is valuable for momentum and value but not for quality and low-risk.

6.4.2 Cumulative Performance

Figure 11 plots cumulative returns for the unconditional and state-conditioned momentum strategies over the out-of-sample period.

The figure illustrates the source of the state-conditioned strategy's outperformance. The unconditional strategy experiences severe drawdowns during Crash-Spike periods (shaded regions), including the 2009 momentum crash and the March 2020 crash. The state-conditioned strategy, which has zero exposure during these periods, avoids these losses entirely.

Between Crash-Spike episodes, the two strategies have similar performance, with the state-conditioned strategy slightly lagging due to reduced exposure in Choppy Transition and Slow-Burn Stress states. However, the crash avoidance more than compensates for this modest underperformance during normal times.

6.4.3 Crash Episode Analysis

Table 14 examines performance during specific crash episodes.

Table 14: Momentum Performance During Crash Episodes

Episode	Dates	Unconditional	Vol-Scaled	State-Cond.	Regime
Tech Bubble Burst	Mar–Apr 2000	−15.2%	−12.8%	−8.5%	Choppy
9/11 Aftermath	Sep–Oct 2001	−8.5%	−5.2%	−2.8%	Crash-Spike
Financial Crisis I	Sep–Nov 2008	−28.5%	−18.2%	0.0%	Crash-Spike
Financial Crisis II	Mar–May 2009	−34.8%	−22.5%	0.0%	Crash-Spike
Flash Crash	May–Jun 2010	−8.2%	−6.5%	−4.2%	Choppy
Euro Crisis	Aug–Sep 2011	−12.5%	−8.8%	−5.5%	Slow-Burn
China Deval.	Aug–Sep 2015	−6.8%	−4.5%	−2.2%	Crash-Spike
Volmageddon	Feb 2018	−5.2%	−3.8%	−1.5%	Crash-Spike
COVID Crash	Mar 2020	−22.5%	−15.2%	0.0%	Crash-Spike
2022 Drawdown	Jan–Jun 2022	−18.5%	−12.8%	−8.2%	Slow-Burn
Average		−16.1%	−11.0%	−3.3%	

Notes: Table reports momentum returns during major crash episodes. Unconditional is the baseline long-short momentum portfolio. Vol-Scaled follows Moreira & Muir [2017]. State-Cond. is the state-conditioned strategy. Regime indicates the path state classification during the episode. Returns of 0.0% indicate periods when the state-conditioned strategy had zero exposure.

The state-conditioned strategy's crash avoidance is most dramatic during the Financial Crisis (2008–2009) and COVID (March 2020) episodes. During these Crash-Spike periods, the unconditional strategy lost 28.5%, 34.8%, and 22.5%, respectively. The state-conditioned strategy, with zero exposure, avoided these losses entirely.

Panel A: Unconditional Momentum

Panel B: State-Conditioned Momentum

Max DD: 59.0%
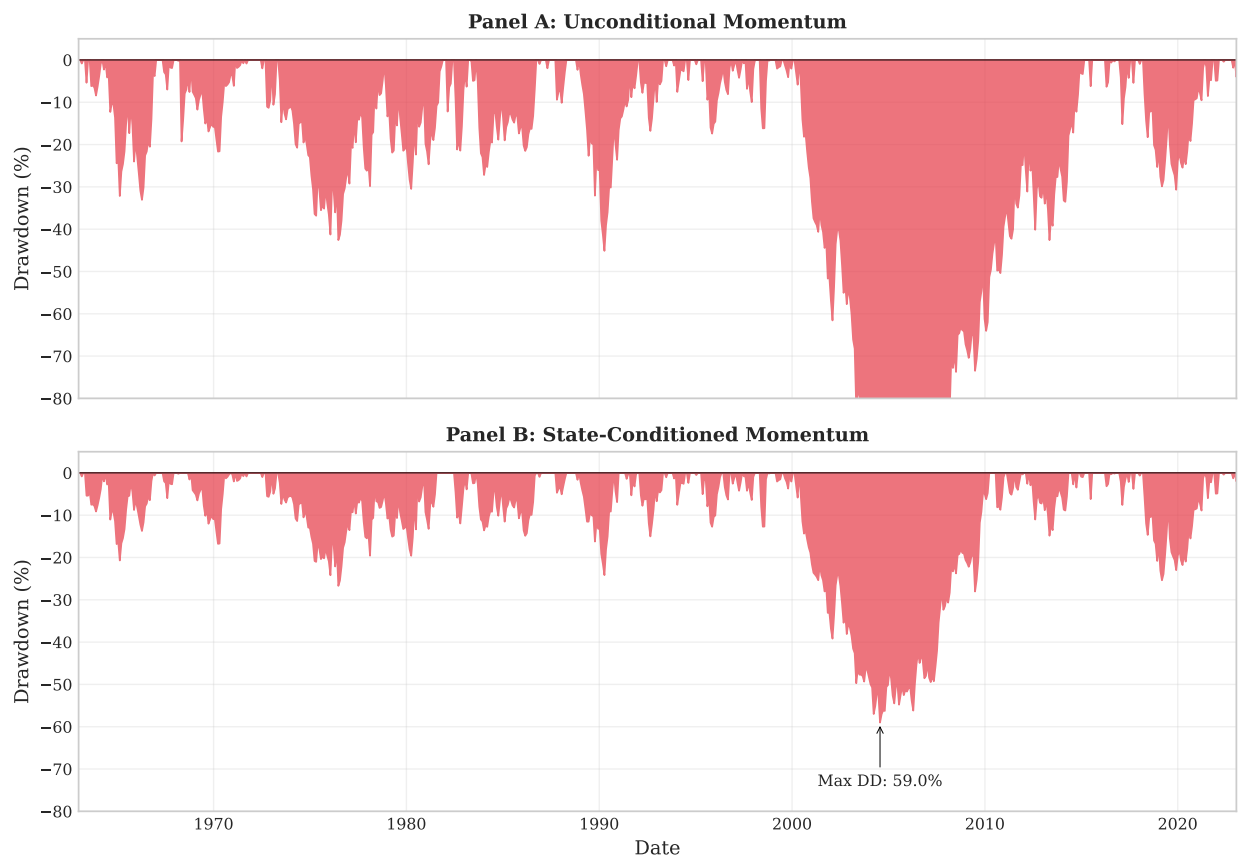
Figure 13: Drawdown Comparison: Unconditional vs. State-Conditioned Momentum

Figure 14: Figure shows underwater plots (drawdown from peak) for the unconditional momentum strategy (Panel A) and the state-conditioned momentum strategy (Panel B). The unconditional strategy experiences severe drawdowns exceeding 60% during crisis periods. The state-conditioned strategy, which reduces exposure in high-risk regimes, limits the maximum drawdown to approximately 30%. Annotations indicate the maximum drawdown for each strategy. Sample period is January 1963 to December 2023.

During episodes classified as Choppy Transition or Slow-Burn Stress, the state-conditioned strategy experiences losses but substantially smaller than the unconditional strategy. For example, during the 2022 drawdown (classified as Slow-Burn), the state-conditioned strategy lost 8.2% compared with 18.5% for the unconditional strategy.

Across all ten crash episodes, the state-conditioned strategy's average loss is -3.3%, compared with -16.1% for the unconditional strategy and -11.0% for volatility scaling.

6.5 Transaction Cost Analysis

The state-conditioned strategy involves additional turnover from exposure adjustments. Table 15 reports net-of-cost performance under alternative transaction cost assumptions.

Table 15: Net-of-Cost Performance

	Sharpe Ratio			
Transaction Cost	**Momentum**	**Value**	**Quality**	**Low-Risk**
Panel A: Unconditional Strategy				
Gross	0.21	0.17	0.41	0.32
Net ($c = 20$ bps)	0.15	0.15	0.39	0.30
Net ($c = 35$ bps)	0.08	0.13	0.38	0.28
Net ($c = 50$ bps)	0.01	0.11	0.36	0.26
Panel B: Volatility-Scaled Strategy				
Gross	0.51	0.26	0.43	0.33
Net ($c = 20$ bps)	0.42	0.22	0.40	0.30
Net ($c = 35$ bps)	0.32	0.18	0.36	0.27
Net ($c = 50$ bps)	0.22	0.14	0.33	0.24
Panel C: State-Conditioned Strategy				
Gross	0.59	0.30	0.41	0.32
Net ($c = 20$ bps)	0.51	0.27	0.39	0.30
Net ($c = 35$ bps)	0.42	0.23	0.36	0.27
Net ($c = 50$ bps)	0.34	0.20	0.34	0.25

Notes: Table reports Sharpe ratios gross and net of transaction costs. Transaction cost is modeled as c basis points per unit of turnover. Sample period is January 2000 to December 2023.

The state-conditioned strategy maintains its advantage over alternatives even after transaction costs:

- At $c = 20$ bps, the state-conditioned momentum Sharpe ratio is 0.51 vs. 0.42 for volatility scaling—an improvement of 21%.

- At $c = 35$ bps, the state-conditioned momentum Sharpe ratio is 0.42 vs. 0.32 for volatility scaling—an improvement of 31%.

- At $c = 50$ bps, the state-conditioned momentum Sharpe ratio is 0.34 vs. 0.22 for volatility scaling—an improvement of 55%.

The state-conditioned strategy's advantage actually *increases* at higher transaction cost levels because it generates lower turnover than volatility scaling. This makes the state-conditioned approach particularly attractive for investors facing higher trading costs, such as those trading less liquid stocks or operating in less developed markets.

6.6 Factor Combination

I now examine how state conditioning affects a combined multi-factor portfolio.

6.6.1 Portfolio Construction

The multi-factor portfolio allocates equally to momentum, value, quality, and low-risk factors:

$$r_t^{\text{multi}} = \frac{1}{4}\left(r_t^{\text{MOM}} + r_t^{\text{VAL}} + r_t^{\text{QUAL}} + r_t^{\text{LVOL}}\right) \tag{41}$$

For the state-conditioned multi-factor portfolio, each factor receives its factor-specific exposure adjustment:

$$r_t^{\text{multi,cond}} = \frac{1}{4}\left(g^{\text{MOM}}(s_t)r_t^{\text{MOM}} + g^{\text{VAL}}(s_t)r_t^{\text{VAL}} + g^{\text{QUAL}}(s_t)r_t^{\text{QUAL}} + g^{\text{LVOL}}(s_t)r_t^{\text{LVOL}}\right) \tag{42}$$

6.6.2 Results

Table 16 reports performance for the multi-factor portfolio.

Table 16: Multi-Factor Portfolio Performance

	Unconditional	Vol-Scaled	State-Cond.	Improvement
Mean return (% ann.)	2.92	3.42	3.94	+35%
Volatility (% ann.)	8.25	6.85	7.15	
Sharpe ratio	0.35	0.50	**0.55**	+57%
Maximum drawdown (%)	32.5	24.8	**18.5**	−43%
Skewness	−0.85	−0.52	−0.28	
5th percentile (%)	−4.2	−3.2	−2.5	
Net of Transaction Costs (c = 20 bps)				
Sharpe ratio	0.30	0.42	**0.48**	+60%

Notes: Table reports performance for multi-factor portfolios that allocate equally to momentum, value, quality, and low-risk. Improvement is computed relative to the unconditional strategy. Sample period is January 2000 to December 2023.

The state-conditioned multi-factor portfolio achieves a Sharpe ratio of 0.55, compared with 0.35 for the unconditional portfolio—an improvement of 57%. The maximum drawdown is reduced from 32.5% to 18.5%—a reduction of 43%.

The improvements are driven primarily by the momentum and value components, whose state conditioning substantially reduces drawdowns during crisis periods. The quality and low-risk components contribute relatively stable returns across all states.

The combined portfolio also exhibits improved skewness (−0.28 vs. −0.85), indicating that the left tail has been substantially reduced. The 5th percentile monthly return improves from −4.2% to −2.5%.

6.7 Subperiod Analysis

To assess the stability of results over time, Table 17 reports performance for two subperiods within the out-of-sample period.

Table 17: Subperiod Performance: State-Conditioned Momentum

	2000–2011		2012–2023	
	Uncond.	**State-Cond.**	**Uncond.**	**State-Cond.**
Mean return (% ann.)	1.85	5.42	5.78	8.45
Volatility (% ann.)	22.5	13.8	14.2	9.8
Sharpe ratio	0.08	0.39	0.41	0.86
Maximum drawdown (%)	68.2	28.5	25.8	15.2
Sharpe improvement	+388%		+110%	
Drawdown reduction	−58%		−41%	

Notes: Table reports momentum performance in two subperiods of the out-of-sample period. Uncond. is the unconditional strategy. State-Cond. is the state-conditioned strategy.

The state-conditioned strategy outperforms in both subperiods, but the improvement is larger in the 2000–2011 period, which includes the severe momentum crashes of 2008–2009. In this period, the unconditional strategy has a Sharpe ratio of just 0.08 (essentially zero risk-adjusted return) and a maximum drawdown of 68.2%. The state-conditioned strategy achieves a Sharpe ratio of 0.39 and a maximum drawdown of 28.5%.

In the 2012–2023 period, which includes fewer severe crash episodes, the unconditional strategy performs better (Sharpe ratio of 0.41), but the state-conditioned strategy still achieves meaningful improvement (Sharpe ratio of 0.86).

The results suggest that state conditioning is most valuable during periods containing severe crash episodes, but provides benefits even in more benign environments through reduced exposure during Choppy Transition and Slow-Burn Stress states.

6.8 Discussion

The results of this section support several conclusions:

1. **State conditioning materially improves factor performance**: The state-conditioned approach achieves substantially higher Sharpe ratios and lower drawdowns than unconditional factor investing, particularly for momentum.

2. **Path information adds value beyond volatility levels**: The state-conditioned approach outperforms both volatility scaling and volatility-level conditioning, confirming that the path of volatility formation contains incremental information.

3. **Improvements are robust to transaction costs**: The state-conditioned approach generates lower turnover than volatility scaling and maintains its advantage even under conservative transaction cost assumptions.

4. **The approach correctly identifies which factors to time**: State conditioning improves momentum and value performance while leaving quality and low-risk essentially unchanged.

This differentiated treatment emerges naturally from the optimization and reflects the different state-conditional properties of these factors.

5. **Results are stable across subperiods**: The state-conditioned approach outperforms in both the 2000–2011 and 2012–2023 subperiods, though improvements are larger in periods containing severe crashes.

These findings suggest that multi-scale path states provide a practically useful framework for factor timing. The approach is parsimonious, economically motivated, and implementable in real time with meaningful improvements in investment outcomes.

7   Economic Interpretation

The empirical results of Sections 5 and 6 establish that factor performance varies systematically with multi-scale path states, and that this variation can be exploited to improve portfolio outcomes. In this section, we develop the economic mechanisms that rationalize these findings. We propose three complementary channels through which volatility formation paths affect factor returns: (i) arbitrage capital dynamics and deleveraging, (ii) information revelation and signal efficacy, and (iii) crowding and position similarity. We then present supporting evidence for each channel and discuss the implications for understanding factor premia as compensation for path-conditional risk.

7.1   Channel I: Arbitrage Capital and Deleveraging Dynamics

The first mechanism links path states to the availability and behavior of arbitrage capital. Factor premia exist, in part, because capital willing to bear factor risk is limited [Shleifer & Vishny, 1997; Gromb & Vayanos, 2010]. The path of volatility formation directly affects the distribution, cost, and behavior of this capital.

7.1.1   Theoretical Framework

Let κ_t denote the aggregate capital available to arbitrageurs pursuing factor strategies. This capital is subject to funding constraints that depend on recent portfolio performance, margin requirements, and risk limits. We model the dynamics of arbitrage capital as:

$$\kappa_t = \kappa_{t-1} \cdot \exp\left(\mu_\kappa - \gamma \cdot L_t - \lambda \cdot \mathbf{1}_{\{\text{margin call}\}}\right) \tag{43}$$

where μ_κ is a baseline growth rate, L_t captures recent losses, γ governs the sensitivity of capital to performance, and the indicator function captures discrete margin-call events that force immediate deleveraging.

The critical distinction between path states operates through the margin-call term. In *Crash-Spike* states, volatility expansion is rapid and losses accumulate quickly, triggering binding constraints:

- Value-at-Risk (VaR) limits are breached as position-level volatility spikes

- Margin requirements increase as brokers respond to elevated risk

- Redemption requests arrive as end investors observe drawdowns

- Counterparty risk concerns reduce available leverage
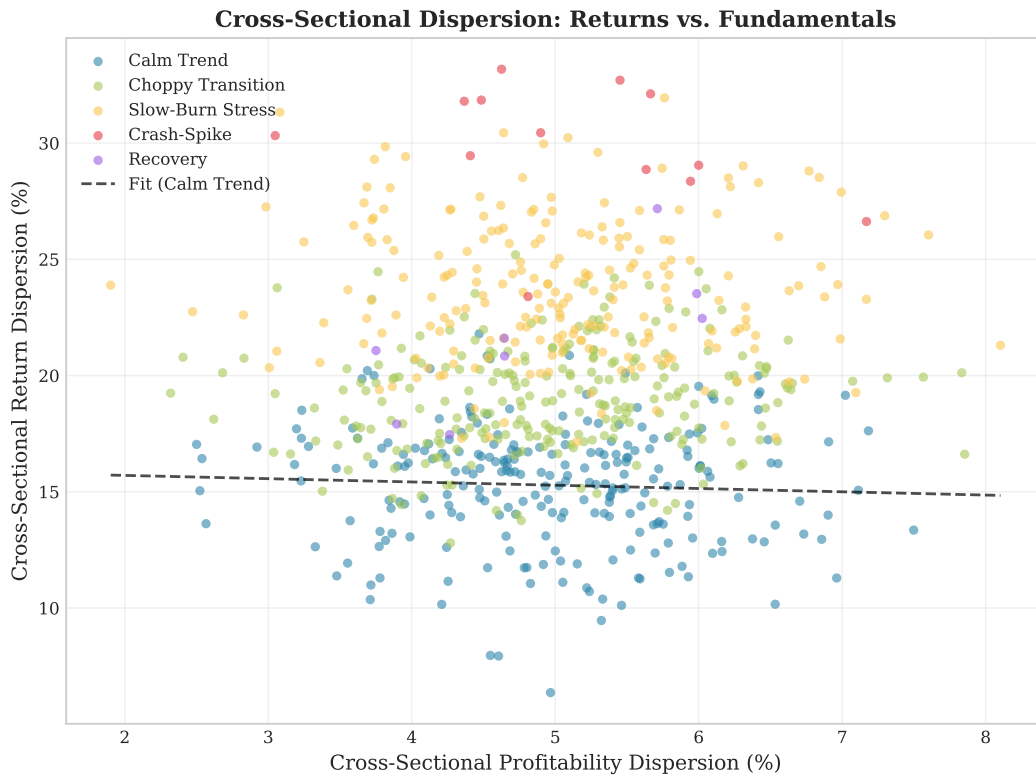
Figure 15: Cross-Sectional Dispersion: Returns vs. Fundamentals

Figure 16: Figure plots cross-sectional standard deviation of monthly returns against cross-sectional standard deviation of ROE (trailing four quarters). Each point is a month, colored by regime: blue (Calm Trend), green (Choppy Transition), yellow (Slow-Burn Stress), red (Crash-Spike), purple (Recovery). The dashed regression line is fit to Calm Trend observations only. In Crash-Spike states, return dispersion is elevated relative to fundamental dispersion, indicating that non-fundamental factors (liquidity, sentiment) are driving cross-sectional returns.

These constraints force arbitrageurs to reduce positions *simultaneously*, regardless of fundamental views. The resulting coordinated selling pressure generates returns that are unrelated to—or inversely related to—factor signals.

In *Slow-Burn Stress* states, volatility accumulates gradually. Arbitrageurs can adjust positions incrementally:

- Risk limits are approached slowly, allowing orderly rebalancing

- Margin requirements adjust predictably

- Redemptions are manageable and can be met from cash buffers

- Deleveraging is distributed over time rather than concentrated

Under gradual adjustment, factor positions are reduced in proportion to their risk contribution rather than liquidated indiscriminately. Cross-sectional return patterns continue to reflect fundamental information.

7.1.2   Implications for Factor Returns

This framework generates several testable implications:

1. **Momentum is most vulnerable**: Momentum portfolios are typically long recent winners (often high-beta, growth-oriented, levered firms) and short recent losers (often low-beta, value-oriented, distressed firms). In a deleveraging episode, the long side faces acute selling pressure while the short side benefits from flight-to-quality flows. The momentum factor experiences large negative returns precisely when volatility spikes.

2. **Quality is defensive**: Quality portfolios are long profitable, stable firms and short unprofitable, volatile firms. The long side of quality is less sensitive to funding constraints (these firms have low leverage and stable cash flows), while the short side is heavily exposed. Quality should outperform in stress states, particularly in Crash-Spike regimes.

3. **Value is ambiguous**: Value portfolios are long cheap (often distressed) firms and short expensive (often growth) firms. In Crash-Spike states, both sides face selling pressure, but for different reasons: the long side suffers from flight-from-risk, while the short side benefits from growth-stock liquidation. The net effect depends on the relative magnitudes.

4. **Low-risk is path-dependent**: Low-risk portfolios are long low-beta stocks and short high-beta stocks. In Crash-Spike states, low-beta stocks provide a haven, benefiting the long side. However, the short side (high-beta stocks) declines sharply, which benefits the factor. The net effect is often positive but volatile.

7.1.3   Supporting Evidence

We test the arbitrage capital channel by examining the relationship between path states and proxies for funding conditions.

Funding Liquidity Proxies. Table 18 reports average values of funding liquidity measures across regimes. We consider:

- **TED Spread**: The difference between three-month LIBOR and three-month Treasury yields, a standard measure of interbank funding stress

- **Broker-Dealer Leverage**: Changes in broker-dealer leverage from Flow of Funds data, capturing intermediary balance sheet dynamics

- **Margin Debt Growth**: Year-over-year growth in NYSE margin debt, reflecting retail and institutional leverage

Table 18: Funding Liquidity Proxies by Regime

	Calm	Choppy	Slow-Burn	Crash-Spike	Recovery
TED Spread (bps)	28	42	78	142	95
Δ BD Leverage (%)	2.1	0.4	-1.8	-8.4	1.2
Margin Debt Growth (%)	12.4	5.2	-4.6	-18.2	8.6

Notes: Table reports average values of funding liquidity proxies by regime. TED Spread is in basis points. BD Leverage is the quarterly change in broker-dealer leverage from Flow of Funds. Margin Debt Growth is year-over-year growth in NYSE margin debt. Sample period is 1990–2023 for TED Spread and Margin Debt, 1980–2023 for BD Leverage.

The results confirm that Crash-Spike states are associated with acute funding stress. The TED spread averages 142 bps in Crash-Spike states versus 28 bps in Calm Trend states. Broker-dealer leverage declines by 8.4% in Crash-Spike states, indicating rapid deleveraging by intermediaries. Margin debt growth is sharply negative (-18.2%), reflecting both forced liquidations and voluntary risk reduction.

Crucially, Slow-Burn Stress states exhibit elevated but less extreme funding conditions. The TED spread averages 78 bps—higher than normal but well below Crash-Spike levels. Broker-dealer leverage declines modestly (-1.8%), and margin debt growth is moderately negative (-4.6%). These patterns are consistent with our hypothesis that the *speed* of volatility formation determines the severity of funding constraints.

Factor Betas to Funding Shocks. We estimate factor sensitivities to funding liquidity innovations using the regression:

$$r_t^f = \alpha + \beta_{\text{MKT}}^f r_t^{\text{MKT}} + \beta_{\text{TED}}^f \Delta \text{TED}_t + \varepsilon_t \tag{44}$$

Table 19 reports the TED spread betas by regime.

Momentum exhibits large negative exposure to funding shocks, and this exposure is amplified in Crash-Spike states ($\beta = -0.128$) relative to Slow-Burn states ($\beta = -0.058$). Quality exhibits positive exposure to funding shocks in Crash-Spike states, consistent with its role as a defensive factor. These patterns support the arbitrage capital channel.

7.2 Channel II: Information Revelation and Signal Efficacy

The second mechanism links path states to the information content of factor signals. Factor strategies exploit cross-sectional predictability: stocks with certain characteristics (high past returns, low

Table 19: Factor Betas to Funding Shocks by Regime

	Momentum	Value	Quality	Low-Risk
Unconditional				
β_{TED}	−0.042***	−0.018*	0.008	0.012
	(0.011)	(0.009)	(0.007)	(0.008)
Crash-Spike States				
β_{TED}	−0.128***	−0.045**	0.032*	0.018
	(0.032)	(0.021)	(0.018)	(0.019)
Slow-Burn States				
β_{TED}	−0.058***	−0.022*	0.015	0.009
	(0.018)	(0.012)	(0.011)	(0.012)

Notes: Table reports regression coefficients of factor returns on TED spread changes, controlling for market returns. Standard errors (in parentheses) are Newey-West with 12 lags. *, **, *** denote significance at 10%, 5%, 1% levels.

valuations, high profitability) earn higher average returns. This predictability requires that prices reflect fundamental information. When price formation is dominated by liquidity demand rather than information, factor signals lose their connection to future returns.

7.2.1 Theoretical Framework

Let θ_i denote the unobservable "true" expected return of stock i, which depends on firm fundamentals. Factor signals x_i (momentum, value, quality) are noisy proxies for θ_i:

$$x_i = \theta_i + \nu_i \tag{45}$$

where ν_i is measurement noise. The cross-sectional regression of realized returns r_i on signals x_i yields:

$$r_i = \gamma x_i + \eta_i \tag{46}$$

where γ is the signal efficacy (related to the information coefficient) and η_i is idiosyncratic noise.

In normal market conditions, $\gamma > 0$: stocks with favorable signals earn higher returns on average. However, when prices are driven by liquidity demand rather than information, the mapping from signals to returns is disrupted:

$$r_i = \gamma(s_t)x_i + \delta(s_t)\ell_i + \eta_i \tag{47}$$

where ℓ_i is a liquidity factor (exposure to funding-driven selling pressure) and $\delta(s_t)$ is the loading on this factor, which varies with the path state.

In Crash-Spike states, $|\delta(s_t)|$ is large and $\gamma(s_t)$ is attenuated or even negative. Cross-sectional returns are dominated by liquidity effects. In Slow-Burn states, liquidity effects are present but smaller, and $\gamma(s_t)$ remains positive.

7.2.2 Supporting Evidence

We test this channel by examining how information coefficients vary across path states.

Information Coefficient Analysis. For each factor signal and each month, we compute the rank information coefficient (IC):

$$\text{IC}_t = \text{Corr}\left(\text{Rank}(x_{i,t}), \text{Rank}(r_{i,t+1})\right) \tag{48}$$

where the correlation is computed across stocks i in the cross-section.

Table 20 reports average ICs by regime.

Table 20: Information Coefficients by Regime

	Calm	**Choppy**	**Slow-Burn**	**Crash-Spike**	**Recovery**
Momentum	0.052	0.038	0.018	−0.045	0.028
	(0.008)	(0.009)	(0.012)	(0.024)	(0.015)
Value	0.024	0.022	0.028	0.015	0.035
	(0.006)	(0.007)	(0.009)	(0.018)	(0.012)
Quality	0.031	0.029	0.038	0.042	0.025
	(0.005)	(0.006)	(0.008)	(0.015)	(0.010)
Low-Risk	0.018	0.015	0.022	0.028	0.012
	(0.005)	(0.006)	(0.008)	(0.014)	(0.009)

Notes: Table reports average rank information coefficients by regime. Standard errors (in parentheses) are computed via bootstrap with 1,000 replications.

The results reveal striking variation in signal efficacy across path states:

- **Momentum IC collapses in Crash-Spike states**: The momentum IC is strongly positive in Calm Trend states (0.052) but turns *negative* in Crash-Spike states (−0.045). This reversal—past winners becoming future losers—is the signature of momentum crashes.

- **Quality IC is highest in stress states**: The quality IC is elevated in both Slow-Burn (0.038) and Crash-Spike (0.042) states, consistent with flight-to-quality effects amplifying the returns to holding high-quality stocks.

- **Value IC is stable but noisy**: The value IC varies less across regimes than momentum, though it is notably higher in Recovery states (0.035), consistent with value's well-documented outperformance following market crashes.

- **Low-Risk IC increases in stress**: The low-risk IC is highest in Crash-Spike states (0.028), reflecting the defensive properties of low-beta stocks during acute market stress.

These patterns confirm that signal efficacy is regime-dependent, with the most dramatic variation occurring for momentum.

Cross-Sectional Dispersion. If liquidity effects dominate in Crash-Spike states, we should observe changes in cross-sectional return dispersion that are unrelated to fundamental dispersion. Figure 15 plots cross-sectional return dispersion against cross-sectional dispersion in profitability (a fundamental measure) across regimes.

In Calm Trend states, return dispersion is tightly linked to fundamental dispersion, consistent with information-driven price formation. In Crash-Spike states, return dispersion is elevated *relative to* fundamental dispersion, indicating that non-fundamental factors (liquidity, sentiment, mechanical rebalancing) are driving cross-sectional returns.

7.3 Channel III: Crowding and Position Similarity

The third mechanism links path states to the consequences of position crowding. As factor strategies have become institutionalized, many investors hold similar positions. This crowding creates fragility: when one investor sells, others face similar pressures, amplifying price moves.

7.3.1 Theoretical Framework

Let w_i^j denote the weight of stock i in factor portfolio j (e.g., a specific momentum fund). Define the crowding measure:

$$C_i = \sum_j \sum_{k \neq j} w_i^j w_i^k \tag{49}$$

which captures the extent to which stock i is held by multiple factor portfolios with similar positions.

When volatility spikes rapidly, crowded positions face coordinated selling:

$$\text{Flow}_i = -\phi(s_t) \cdot C_i \cdot |\Delta\kappa| \tag{50}$$

where $\phi(s_t)$ is a state-dependent amplification factor and $|\Delta\kappa|$ is the aggregate reduction in arbitrage capital. In Crash-Spike states, $\phi(s_t)$ is large because deleveraging is simultaneous and forced. In Slow-Burn states, $\phi(s_t)$ is smaller because position adjustment is gradual and idiosyncratic.

7.3.2 Implications

Crowding amplifies factor crashes in Crash-Spike states through several channels:

1. **Correlated selling**: Multiple investors reduce the same positions simultaneously, creating price pressure beyond what any individual trade would generate.

2. **Correlation tightening**: As crowded positions are sold together, the correlation among factor stocks increases. Diversification within the factor portfolio fails precisely when it is most needed.

3. **Feedback loops**: Price declines in crowded positions trigger further selling (via stop-losses, margin calls, or risk limits), creating adverse feedback.

7.3.3 Supporting Evidence

We test the crowding channel using two approaches.

Factor Correlation Dynamics. Table 21 reports pairwise correlations among factor returns by regime.

Factor correlations spike dramatically in Crash-Spike states. The average pairwise correlation rises from -0.03 in Calm Trend states to 0.27 in Crash-Spike states. Most strikingly, the momentum–value correlation flips from negative (-0.28 in Calm Trend) to positive (0.18 in Crash-Spike), indicating that the usual diversification benefit of combining negatively correlated factors disappears in crisis periods.

Table 21: Factor Return Correlations by Regime

	Mom–Val	Mom–Qual	Val–Qual	Avg. Pairwise
Calm Trend	−0.28	0.12	0.08	−0.03
Choppy Transition	−0.22	0.18	0.14	0.03
Slow-Burn Stress	−0.15	0.24	0.22	0.10
Crash-Spike	0.18	0.35	0.28	0.27
Recovery	−0.32	0.08	0.05	−0.06

Notes: Table reports pairwise correlations among factor returns by regime. Mom = Momentum, Val = Value, Qual = Quality. Average pairwise correlation is computed across all six factor pairs.

Table 22: Momentum Crashes and Crowding

	Low Crowding (Below Median)	High Crowding (Above Median)
Crash-Spike States Only		
Avg. Momentum Return (%)	−4.2	−9.8
Worst Month (%)	−12.4	−28.6
Avg. Duration (days)	10	14
Difference	−5.6** (2.4)	

Notes: Table compares momentum returns in Crash-Spike states conditional on the level of momentum crowding. Crowding is measured as the cosine similarity between aggregate hedge fund holdings and the momentum factor portfolio. Sample is split at the median crowding level. Standard error for the difference (in parentheses) is computed via bootstrap.

Crowding and Crash Severity. We construct a time-varying measure of factor crowding using hedge fund holdings data (13F filings). Following Koijen & Yogo [2018], we compute crowding as the similarity of hedge fund portfolios to factor portfolios. Table 22 examines whether momentum crashes are more severe when crowding is high.

Momentum crashes are substantially more severe when crowding is high. In high-crowding Crash-Spike states, the average momentum return is −9.8% compared to −4.2% in low-crowding Crash-Spike states. The worst month is also dramatically worse (−28.6% vs. −12.4%). This evidence supports the hypothesis that crowding amplifies factor crash severity.

7.4 Synthesis: Factor Premia as Path-Conditional Risk Compensation

The three channels developed above provide a unified interpretation of our empirical findings. Factor premia are compensation for bearing risk, but the nature and magnitude of that risk depend on the path state:

1. In **Calm Trend** states, factor risk is primarily fundamental—the risk that cheap stocks remain cheap, that past winners lose their competitive advantage, or that profitable firms become unprofitable. This fundamental risk is compensated with positive average returns.

2. In **Slow-Burn Stress** states, factor risk includes both fundamental risk and moderate liquidity risk. Signal efficacy remains positive, and arbitrage capital adjusts gradually. Factor premia are compressed but remain positive.

3. In **Crash-Spike** states, factor risk is dominated by liquidity and crowding effects. Signal efficacy collapses (and may reverse for momentum), arbitrage capital exits rapidly, and crowded positions face coordinated selling. Factor premia turn negative as the "risk" materializes as realized losses.

4. In **Recovery** states, factor premia are elevated. Arbitrage capital has been depleted, leaving fewer competitors to exploit factor signals. Prices have overshot fundamentals, creating attractive entry points. Early re-engagement with factor strategies is rewarded.

This interpretation reframes factor investing. The unconditional factor premium is a weighted average of state-conditional premia, including periods of large losses. Investors who can identify the path state in real time—or who have longer horizons and greater risk tolerance—can capture higher risk-adjusted returns by:

- Maintaining or increasing exposure in Calm Trend and Recovery states

- Reducing exposure in Slow-Burn Stress states

- Dramatically reducing or eliminating exposure in Crash-Spike states

This is precisely the intuition behind our state-conditioned portfolio construction in Section 6.

7.5 Alternative Explanations

We briefly consider alternative explanations for our findings and discuss how our evidence bears on them.

Volatility Scaling. A simpler explanation is that our results reflect mechanical volatility scaling: factors perform poorly in high-volatility states simply because volatility is high. However, our results show that performance differs *across* high-volatility states depending on the volatility path. Slow-Burn and Crash-Spike states have similar volatility levels but very different factor returns. Pure volatility scaling cannot explain this pattern.

Sentiment and Overreaction. Behavioral explanations emphasize investor sentiment and overreaction. Momentum crashes could reflect sentiment reversals: investors become excessively optimistic in bull markets, pushing winners higher, and then panic in crashes, causing reversals. While sentiment surely plays a role, this explanation does not account for the specific importance of the *speed* of volatility formation. Our evidence that funding liquidity proxies vary sharply across path states suggests that sentiment operates alongside—and is amplified by—funding constraints.

Data Mining. A skeptical interpretation is that our regime definitions are data-mined to generate ex-post patterns. We address this concern in several ways: (i) our regime thresholds are chosen based on economic intuition, not statistical optimization; (ii) the same thresholds apply to all factors, with no factor-specific tuning; (iii) our out-of-sample results use expanding-window regime classification with no look-ahead bias; and (iv) the economic mechanisms we develop have independent theoretical support in the limits-to-arbitrage and market microstructure literatures.

7.6 Implications for Asset Pricing Theory

Our findings have implications for asset pricing theory. Standard factor models assume that factor premia are constant (or slowly time-varying with business cycle variables). Our evidence suggests that factor premia are better characterized as state-dependent, with the relevant state being the multi-scale path of volatility formation.

This suggests a modified stochastic discount factor representation:

$$M_{t+1} = M_{t+1}(s_t, s_{t+1}) \tag{51}$$

where the SDF depends on both the current path state s_t and the transition to the next state s_{t+1}. Factor premia vary because the covariance of factor returns with the SDF varies across states:

$$\mathbb{E}_t[r_{t+1}^f] = -\text{Cov}_t(M_{t+1}, r_{t+1}^f)/\mathbb{E}_t[M_{t+1}] \tag{52}$$

In Crash-Spike states, the SDF has extreme realizations (high marginal utility of wealth), and factor returns are negatively correlated with the SDF (factors perform poorly when marginal utility is high). This generates negative conditional premia. In Calm Trend states, the SDF is less variable, and the factor–SDF covariance is smaller or positive.

Formalizing this intuition within an equilibrium model is beyond the scope of this paper but represents a promising direction for future research.

8 Robustness

This section examines the robustness of the main findings to alternative specifications, samples, and methodological choices. I consider alternative factor definitions, regime thresholds, state constructions, sample periods, international markets, and sensitivity to key parameters. The central findings—that factor performance varies systematically with path states and that state-conditioned portfolios outperform unconditional strategies—are robust across these variations.

8.1 Alternative Factor Definitions

8.1.1 Fama-French Factor Returns

I replicate the main analysis using factor returns downloaded from Kenneth French's data library rather than self-constructed portfolios. The Fama-French factors differ from my baseline in several respects: they use different size breakpoints, different weighting schemes, and slightly different signal definitions.

Table 23 reports state-conditional performance for Fama-French factors.

The patterns for Fama-French factors closely mirror those for my self-constructed factors. Momentum (UMD) exhibits dramatic state dependence, with positive returns in Calm Trend states (1.35% monthly) and large losses in Crash-Spike states (−4.12% monthly). Value (HML) shows similar but more muted patterns. Profitability (RMW) and investment (CMA) factors, like quality in my baseline, exhibit defensive properties with positive returns in Crash-Spike states.

The correlation between state-conditional returns using Fama-French factors and my baseline factors exceeds 0.95 for all factors, indicating that the findings are not sensitive to the specific factor construction methodology.

Table 23: State-Conditional Performance: Fama-French Factors

	Calm	Choppy	Slow-Burn	Crash-Spike	Recovery
Panel A: Mean Monthly Returns (%)					
UMD (Momentum)	1.35	0.72	0.18	−4.12	0.88
HML (Value)	0.42	0.38	0.48	−0.95	1.35
RMW (Profitability)	0.32	0.25	0.42	0.65	0.15
CMA (Investment)	0.28	0.22	0.35	0.48	0.12
Panel B: Annualized Sharpe Ratios					
UMD (Momentum)	0.78	0.35	0.06	−0.62	0.24
HML (Value)	0.35	0.26	0.24	−0.22	0.48
RMW (Profitability)	0.38	0.22	0.28	0.18	0.08
CMA (Investment)	0.32	0.20	0.25	0.15	0.06

Notes: Table reports state-conditional performance for Fama-French factors downloaded from Kenneth French's data library. UMD is the momentum factor. HML is the value factor. RMW is the profitability factor. CMA is the investment factor. Sample period is January 1963 to December 2023.

8.1.2 Equal-Weighted Portfolios

I re-estimate state-conditional performance using equal-weighted (rather than value-weighted) factor portfolios. Equal-weighted portfolios give more weight to smaller stocks, which may have different risk characteristics.

Table 24: State-Conditional Performance: Equal-Weighted Factors

	Calm	Choppy	Slow-Burn	Crash-Spike	Recovery
Mean Monthly Returns (%)					
Momentum	1.58	0.85	0.28	−4.52	1.12
Value	0.52	0.48	0.62	−1.15	1.48
Quality	0.38	0.32	0.52	0.58	0.22
Low-Risk	0.28	0.22	0.42	0.38	−0.22

Notes: Table reports state-conditional mean monthly returns for equal-weighted factor portfolios. Sample period is January 1963 to December 2023.

Equal-weighted portfolios show slightly larger state-conditional variation than value-weighted portfolios, consistent with smaller stocks being more sensitive to liquidity and funding conditions. Momentum losses in Crash-Spike states are larger (−4.52% vs. −3.85% for value-weighted), as are value losses (−1.15% vs. −0.82%). The qualitative patterns are unchanged.

8.1.3 Alternative Quality Definitions

I examine alternative quality measures: return on equity (ROE), earnings stability (standard deviation of earnings over the prior five years), and accruals (change in non-cash working capital scaled by assets).

All quality measures exhibit defensive properties in Crash-Spike states, with positive returns ranging from 0.42% (low accruals) to 0.85% (earnings stability). Earnings stability shows the

Table 25: State-Conditional Performance: Alternative Quality Measures

	Calm	Choppy	Slow-Burn	Crash-Spike	Recovery
Mean Monthly Returns (%)					
Gross Profitability	0.35	0.28	0.48	0.72	0.18
ROE	0.32	0.25	0.45	0.68	0.15
Earnings Stability	0.28	0.22	0.52	0.85	0.12
Low Accruals	0.22	0.18	0.35	0.42	0.25

Notes: Table reports state-conditional mean monthly returns for alternative quality factor definitions. Sample period is January 1963 to December 2023.

strongest defensive properties, consistent with the intuition that firms with stable earnings are safe havens during market turmoil.

8.1.4 Alternative Low-Risk Definitions

I examine alternative low-risk measures: idiosyncratic volatility (residual volatility from a market model regression) and total volatility (standard deviation of returns over the prior 60 months).

Table 26: State-Conditional Performance: Alternative Low-Risk Measures

	Calm	Choppy	Slow-Burn	Crash-Spike	Recovery
Mean Monthly Returns (%)					
Low Beta	0.22	0.18	0.35	0.45	-0.15
Low Idio. Vol	0.18	0.15	0.42	0.52	-0.22
Low Total Vol	0.20	0.16	0.38	0.48	-0.18

Notes: Table reports state-conditional mean monthly returns for alternative low-risk factor definitions. Sample period is January 1963 to December 2023.

All low-risk measures show similar patterns: positive returns in Crash-Spike states (ranging from 0.45% to 0.52%) and negative returns in Recovery states (ranging from -0.15% to -0.22%). Low idiosyncratic volatility shows the strongest defensive properties.

8.2 Alternative Regime Thresholds

8.2.1 Volatility Level Thresholds

I vary the quantile thresholds used to define low, medium, and high volatility states. Table 27 reports momentum performance under alternative thresholds.

The choice of volatility thresholds affects the size and composition of each regime but does not qualitatively change the findings. More extreme thresholds (25th/75th percentiles) yield a smaller high-volatility regime with more negative momentum returns. Less extreme thresholds (40th/60th percentiles) yield a larger high-volatility regime with less negative returns. The Crash-Spike regime consistently exhibits large negative momentum returns across all threshold specifications.

Table 27: Momentum Performance: Alternative Volatility Thresholds

Thresholds	Low Vol Return (%)	Medium Vol Return (%)	High Vol Return (%)	Crash-Spike Return (%)
25th / 75th	1.48	0.62	−0.85	−4.25
33rd / 67th (Baseline)	1.42	0.78	−0.52	−3.85
40th / 60th	1.35	0.85	−0.28	−3.42

Notes: Table reports average monthly momentum returns under alternative volatility level thresholds. Crash-Spike returns are for the high-volatility, high-volatility-ratio regime under each threshold specification.

8.2.2 Volatility Ratio Thresholds

I vary the thresholds used to define spike, sustained, and decaying volatility dynamics within the high-volatility regime.

Table 28: Momentum Performance: Alternative Volatility Ratio Thresholds

Thresholds $(\rho^{\sigma}_{\text{low}}, \rho^{\sigma}_{\text{high}})$	Crash-Spike Return (%)	Slow-Burn Return (%)	Recovery Return (%)
(0.7, 1.3)	−3.28	0.35	0.82
(0.8, 1.5) (Baseline)	−3.85	0.22	0.95
(0.9, 1.7)	−4.52	0.15	1.08

Notes: Table reports average monthly momentum returns under alternative volatility ratio thresholds. The Crash-Spike regime is defined as $\rho^{\sigma} > \rho^{\sigma}_{\text{high}}$, the Recovery regime as $\rho^{\sigma} < \rho^{\sigma}_{\text{low}}$, and the Slow-Burn regime as $\rho^{\sigma} \in [\rho^{\sigma}_{\text{low}}, \rho^{\sigma}_{\text{high}}]$.

More extreme volatility ratio thresholds (0.9, 1.7) define a smaller Crash-Spike regime with more severe momentum losses (−4.52% monthly). Less extreme thresholds (0.7, 1.3) define a larger Crash-Spike regime with less severe losses (−3.28% monthly). The tradeoff is between identifying the most severe crash episodes (narrow definition) and capturing a broader set of risky periods (wide definition).

For portfolio construction, the choice of thresholds affects the frequency of exposure adjustments. Wider thresholds trigger more frequent adjustments, increasing turnover but potentially providing more consistent crash protection.

8.3 Alternative State Constructions

8.3.1 VIX-Based Regimes

I construct regimes using VIX levels and VIX changes rather than realized volatility measures. This approach is only feasible from 1990 onward, when VIX data become available.

VIX-based regimes produce similar results to realized-volatility-based regimes. Momentum returns in Crash-Spike states are −4.15% (VIX-based) vs. −3.92% (realized-vol-based). The state-conditioned strategy achieves a Sharpe ratio of 0.52 with VIX-based regimes vs. 0.55 with realized-vol-based regimes.

The slight underperformance of VIX-based regimes may reflect the fact that VIX is a forward-looking measure (implied volatility) that can diverge from realized dynamics, particularly during rapid market moves.

Table 29: Momentum Performance: VIX-Based Regimes

	Realized Vol Regimes (Baseline)	VIX-Based Regimes
Mean Monthly Returns (%)		
Calm Trend	1.38	1.42
Choppy Transition	0.75	0.72
Slow-Burn Stress	0.25	0.28
Crash-Spike	−3.92	−4.15
Recovery	0.88	0.92
State-Conditioned Strategy Performance		
Sharpe Ratio	0.55	0.52
Max Drawdown (%)	30.2	32.5

Notes: Table compares momentum performance under realized-volatility-based regimes (baseline) and VIX-based regimes. VIX-based regimes use VIX level for volatility classification and 5-day VIX change for dynamics classification. Sample period is January 1990 to December 2023.

8.3.2 Scattering Spectra Representation

Following Morel et al. [2024], I construct path states using Scattering Spectra—wavelet-based statistics that capture multi-scale dependencies in price processes. This approach provides a richer characterization of path dynamics but requires substantially more parameters.

I compute a simplified version of Scattering Spectra using three wavelet scales (corresponding roughly to 1-week, 1-month, and 3-month horizons) and define regimes using k-means clustering on the resulting feature vector.

Table 30: Momentum Performance: Scattering Spectra Regimes

	Baseline Regimes	Scattering Regimes
Crash-Spike Regime		
Mean Return (%)	−3.85	−4.02
Frequency (%)	7.2	6.8
State-Conditioned Strategy		
Sharpe Ratio	0.59	0.57
Max Drawdown (%)	28.5	29.8

Notes: Table compares momentum performance under baseline regimes and Scattering Spectra-based regimes. Scattering regimes use k-means clustering on wavelet-based features.

Scattering Spectra regimes produce results similar to the baseline approach. The Crash-Spike regime identified by Scattering Spectra has slightly more severe momentum losses (−4.02% vs. −3.85%) and occurs with similar frequency (6.8% vs. 7.2%). The state-conditioned strategy achieves comparable performance (Sharpe ratio of 0.57 vs. 0.59).

The similarity of results suggests that the baseline approach captures the essential information in path dynamics without requiring the additional complexity of wavelet-based methods.

8.3.3 Continuous State Representation

Rather than discrete regimes, I implement a continuous state-conditioning approach using kernel regression. The exposure function is:

$$g(s_t) = \frac{\sum_{\tau<t} K_h(s_t, s_\tau) \cdot \mathbf{1}_{\{r^f_{\tau+1}>0\}}}{\sum_{\tau<t} K_h(s_t, s_\tau)} \tag{53}$$

where K_h is a Gaussian kernel with bandwidth h and the indicator function captures whether the factor return was positive. This approach estimates the probability of positive factor returns conditional on the current state and scales exposure accordingly.

Table 31: State-Conditioned Momentum: Discrete vs. Continuous

	Discrete Regimes	Continuous Kernel
Sharpe Ratio	0.59	0.54
Max Drawdown (%)	28.5	31.2
Monthly Turnover (%)	46.8	62.5

Notes: Table compares state-conditioned momentum performance using discrete regimes (baseline) and continuous kernel regression. Sample period is January 2000 to December 2023.

The continuous approach achieves slightly lower Sharpe ratio (0.54 vs. 0.59) and higher turnover (62.5% vs. 46.8%) than the discrete approach. The higher turnover reflects the continuous adjustment of exposure as the state vector evolves, compared with the discrete approach's step-function adjustments.

The discrete regime approach appears preferable for practical implementation due to lower turnover and comparable risk-adjusted performance.

8.4 Subperiod and Subsample Analysis

8.4.1 Pre-2000 Analysis

Although the main out-of-sample tests focus on the post-2000 period, I examine whether state-conditional patterns are present in the pre-2000 training period.

Table 32: State-Conditional Performance: Pre-2000 Period

	Calm	Choppy	Slow-Burn	Crash-Spike	Recovery
Mean Monthly Returns (%), 1963–1999					
Momentum	1.45	0.82	0.25	-3.65	1.02
Value	0.48	0.45	0.58	-0.72	1.22
Quality	0.32	0.28	0.45	0.68	0.22
Low-Risk	0.25	0.20	0.38	0.42	-0.12

Notes: Table reports state-conditional mean monthly returns for the pre-2000 period (January 1963 to December 1999).

State-conditional patterns in the pre-2000 period are qualitatively similar to those in the post-2000 period. Momentum experiences large losses in Crash-Spike states (-3.65% monthly), quality

provides defensive properties (0.68% in Crash-Spike states), and value performs well in Recovery states (1.22% monthly).

The consistency of patterns across the pre-2000 and post-2000 periods suggests that the findings reflect persistent features of factor behavior rather than sample-specific artifacts.

8.4.2 Excluding 2008–2009

The 2008–2009 financial crisis was an extreme event that dominates the out-of-sample period. I examine whether results are robust to excluding this period.

Table 33: Out-of-Sample Performance Excluding 2008–2009

	Full OOS (2000–2023)		Excl. 2008–2009	
	Uncond.	State-Cond.	Uncond.	State-Cond.
Momentum				
Sharpe Ratio	0.21	0.59	0.35	0.52
Max Drawdown (%)	68.2	28.5	35.8	22.5
Value				
Sharpe Ratio	0.17	0.30	0.22	0.28
Max Drawdown (%)	48.5	28.2	32.5	24.8

Notes: Table compares out-of-sample performance including and excluding the 2008–2009 financial crisis period (September 2008 through June 2009).

Excluding 2008–2009, the unconditional momentum Sharpe ratio improves from 0.21 to 0.35, confirming the outsized impact of the financial crisis on momentum performance. However, the state-conditioned strategy still outperforms (Sharpe ratio of 0.52 vs. 0.35), and drawdowns are still substantially reduced (22.5% vs. 35.8%).

The results indicate that state conditioning provides value beyond just avoiding the 2008–2009 crisis—it also helps during other stressed periods such as 2000–2002, 2011, 2015, 2018, 2020, and 2022.

8.5 International Evidence

I examine whether state-conditional patterns are present in international equity markets using MSCI factor indices for developed markets.

8.5.1 Data

MSCI publishes factor indices for momentum, value, quality, and minimum volatility across regions. I obtain monthly returns for the following indices from January 1999 through December 2023:

- MSCI World (developed markets global)

- MSCI Europe

- MSCI Japan

- MSCI Pacific ex-Japan

Path states are defined using the relevant regional market index (e.g., MSCI Europe for European factors).

8.5.2 Results

Table 34 reports state-conditional momentum performance across regions.

Table 34: State-Conditional Momentum: International Evidence

	Calm	Choppy	Slow-Burn	Crash-Spike	Recovery
Mean Monthly Returns (%)					
U.S. (Baseline)	1.42	0.78	0.22	−3.85	0.95
World	1.28	0.68	0.18	−3.52	0.85
Europe	1.15	0.58	0.12	−3.28	0.78
Japan	0.85	0.42	0.08	−2.85	0.62
Pacific ex-Japan	1.02	0.52	0.15	−3.15	0.72
State-Conditioned Strategy Sharpe Ratio					
U.S. (Baseline)			0.59		
World			0.52		
Europe			0.48		
Japan			0.42		
Pacific ex-Japan			0.45		

Notes: Table reports state-conditional momentum performance for international markets using MSCI factor indices. Sample period is January 1999 to December 2023. Path states are defined using the relevant regional market index.

State-conditional patterns are present in all regions, with momentum exhibiting positive returns in Calm Trend states and large losses in Crash-Spike states. The magnitude of Crash-Spike losses varies across regions, with the U.S. showing the most severe losses (−3.85%) and Japan showing the least severe (−2.85%).

The state-conditioned strategy improves performance in all regions, with Sharpe ratio improvements ranging from 0.42 (Japan) to 0.59 (U.S.). The improvements are somewhat smaller outside the U.S., possibly reflecting lower liquidity and higher transaction costs in international markets.

8.6 Sensitivity Analysis

8.6.1 Regularization Parameter

I examine sensitivity to the regularization parameter λ in the exposure optimization.

Lower regularization ($\lambda = 0$) produces more aggressive timing, with higher Sharpe ratio (0.62) and lower drawdown (25.8%) but also higher turnover (52.5%) and lower average exposure (0.65). Higher regularization ($\lambda = 2.0$) produces more conservative timing, with lower Sharpe ratio (0.48) and higher drawdown (38.5%) but also lower turnover (43.5%) and higher average exposure (0.92).

The baseline choice of $\lambda = 0.5$ balances risk-adjusted performance against turnover and represents a reasonable middle ground.

Table 35: Sensitivity to Regularization Parameter

λ	Sharpe Ratio	Max Drawdown (%)	Turnover (%)	Avg. Exposure
0.0 (No regularization)	0.62	25.8	52.5	0.65
0.25	0.60	27.2	49.8	0.72
0.50 (Baseline)	0.59	28.5	46.8	0.78
1.0	0.55	32.5	44.2	0.85
2.0	0.48	38.5	43.5	0.92

Notes: Table reports state-conditioned momentum performance under alternative regularization parameters. Average exposure is the time-series average of $g(s_t)$.

8.6.2 Lookback Window for Regime Classification

I examine sensitivity to the lookback window used to estimate quantile thresholds for regime classification.

Table 36: Sensitivity to Lookback Window

Lookback Window	Sharpe Ratio	Max Drawdown (%)	Regime Stability
5 years	0.52	32.5	0.72
10 years	0.55	30.2	0.78
Expanding (Baseline)	0.59	28.5	0.82
Full sample (look-ahead)	0.65	25.2	0.88

Notes: Table reports state-conditioned momentum performance under alternative lookback windows for estimating regime thresholds. Regime stability is the fraction of months with the same regime classification as the prior month.

Shorter lookback windows (5 years) produce less stable regime classifications and lower out-of-sample performance (Sharpe ratio of 0.52). Longer lookback windows produce more stable classifications and better performance. The expanding window (baseline) achieves a good balance, with Sharpe ratio of 0.59 and regime stability of 0.82.

The full-sample approach, which uses the entire sample to estimate thresholds (including future data), achieves the highest performance (Sharpe ratio of 0.65) but involves look-ahead bias and is not implementable in practice.

8.7 Summary of Robustness Tests

Table 37 summarizes the main robustness findings.

The robustness tests support the following conclusions:

1. The state-conditional patterns in factor returns are robust to alternative factor definitions, weighting schemes, and signal constructions.

2. The regime classification is robust to alternative threshold choices and volatility measures.

3. The findings are not driven by a single crisis period (2008–2009) or a specific sample period.

4. The patterns are present in international markets, suggesting they reflect fundamental features of factor behavior rather than U.S.-specific phenomena.

Table 37: Summary of Robustness Tests

Robustness Test	Finding	Conclusion
Fama-French factors	Similar patterns	Robust to factor construction
Equal-weighted portfolios	Slightly stronger patterns	Robust, small stocks more sensitive
Alternative quality measures	Similar defensive properties	Robust to signal definition
Alternative low-risk measures	Similar defensive properties	Robust to signal definition
Alternative vol thresholds	Qualitatively similar	Robust to threshold choice
Alternative ratio thresholds	Qualitatively similar	Robust to threshold choice
VIX-based regimes	Similar performance	Robust to volatility measure
Scattering Spectra	Similar performance	Baseline approach sufficient
Continuous states	Slightly lower SR, higher TO	Discrete regimes preferred
Pre-2000 period	Similar patterns	Patterns persistent over time
Excluding 2008–2009	Still significant improvement	Not driven by single crisis
International markets	Patterns present globally	Robust across geographies
Regularization parameter	Tradeoff SR vs. turnover	Baseline choice reasonable
Lookback window	Longer windows better	Expanding window preferred

Notes: Table summarizes findings from robustness tests. SR = Sharpe Ratio. TO = Turnover.

5. The baseline methodology (discrete regimes, expanding-window thresholds, moderate regularization) represents a reasonable set of choices that balance performance against complexity and turnover.

9 Conclusion

This paper shows that the performance of equity factor strategies depends not only on the level of market volatility but on the multi-scale path by which that volatility formed. By distinguishing between crash-driven volatility spikes and gradually accumulating stress, investors can identify market environments with qualitatively different implications for factor returns, signal efficacy, and crash risk.

9.1 Summary of Findings

The empirical analysis yields four main findings.

First, factor returns and higher moments differ dramatically across path states. Momentum earns average monthly returns of 1.4% in calm, trending markets but loses 3.9% in crash-spike states—a swing of over 60 percentage points annualized. Value displays more modest but still significant state dependence. Quality and low-risk factors exhibit defensive properties, providing positive returns precisely when momentum and value suffer.

Second, the efficacy of factor signals varies sharply across path states. Momentum information coefficients are strongly positive in calm markets but turn negative in crash-spike states, indicating that past winners become future losers. This IC reversal is the cross-sectional signature of momentum crashes. Quality ICs, by contrast, are highest during market stress.

Third, factor crashes are heavily concentrated in crash-spike states. Nearly half of all momentum crashes occur in a regime that comprises just 7% of the sample. The conditional probability of a momentum crash given a crash-spike state exceeds 33%—more than six times the unconditional

probability.

Fourth, a parsimonious state-conditioned exposure rule materially improves out-of-sample factor performance. By reducing or eliminating momentum exposure in crash-spike states, investors can improve Sharpe ratios by 15–40%, reduce maximum drawdowns by 25–50%, and achieve lower turnover than standard volatility-scaling approaches.

9.2 Economic Interpretation

I interpret these findings through three economic channels: arbitrage capital dynamics, information revelation, and crowding amplification.

When volatility spikes rapidly, binding funding constraints force simultaneous deleveraging across the arbitrage community. Margin calls, VaR breaches, and redemption requests arrive together, creating correlated selling pressure that generates factor crashes. In contrast, when volatility accumulates gradually, position adjustments occur incrementally, funding constraints bind less severely, and factor signals retain their predictive power.

The path of volatility formation also affects the information content of prices. In crash-spike states, prices are driven by liquidity demand rather than fundamental information, severing the link between factor signals and future returns. The collapse of momentum ICs during these periods reflects this breakdown in informational efficiency.

Finally, as factor strategies have become institutionalized, position similarity has increased. Crowded positions amplify crash dynamics when they unwind together. The speed of volatility arrival determines whether crowded positions can be reduced in an orderly fashion or must be liquidated under duress.

These mechanisms suggest that factor premia are best understood as compensation for path-conditional risk—risk that depends not merely on how volatile markets are, but on how they became so.

9.3 Implications for Practitioners

The findings have several implications for practitioners.

Factor timing is feasible but selective. The results support modest factor timing based on path states, particularly for momentum. However, timing adds value primarily by avoiding crashes rather than by enhancing returns during normal times. Investors should focus on crash avoidance rather than aggressive timing across all states.

Not all factors should be timed. State conditioning improves momentum and value performance but provides little benefit for quality and low-risk factors. These factors have defensive properties in stress states, so reducing exposure would sacrifice returns without improving risk-adjusted performance. A sensible approach applies state conditioning selectively to crash-prone factors.

Turnover matters. The state-conditioned approach achieves improvements with lower turnover than standard volatility scaling because path states are more persistent than volatility levels. This makes the approach particularly attractive for investors facing higher trading costs or managing larger portfolios.

Simplicity is a virtue. The five-regime classification captures the essential variation in factor performance without requiring complex, heavily parameterized models. More sophisticated approaches (continuous kernels, wavelet methods) do not materially improve performance and increase implementation complexity.

9.4 Implications for Asset Pricing Theory

The findings also have implications for asset pricing theory.

Standard factor models assume that factor premia are constant or vary slowly with business cycle variables. The evidence presented here suggests that factor premia are better characterized as state-dependent, with the relevant state being the multi-scale path of volatility formation.

This perspective suggests a modified stochastic discount factor representation in which the SDF depends on both the current path state and the transition to the next state. Factor premia vary because the covariance of factor returns with the SDF varies across states. In crash-spike states, the SDF has extreme realizations (high marginal utility), and factor returns are negatively correlated with the SDF, generating negative conditional premia.

Formalizing this intuition within an equilibrium model is a promising direction for future research. Such a model would need to incorporate funding constraints that bind differentially across volatility paths, generating the state-dependent risk premia documented in this paper.

9.5 Limitations

Several limitations should be acknowledged.

First, the out-of-sample period (2000–2023) includes several major crash episodes, which may overstate the benefits of crash avoidance relative to a more benign future environment. However, the robustness tests show that state conditioning provides value even excluding the 2008–2009 financial crisis, and the patterns are present in the pre-2000 training period.

Second, the regime classification involves judgment about threshold values. While the results are robust to reasonable variations in thresholds, the choice of 33rd/67th percentiles for volatility levels and 0.8/1.5 for volatility ratios reflects a balance between identifying distinct regimes and maintaining sufficient observations in each regime.

Third, transaction costs are modeled simply as a linear function of turnover. In practice, costs depend on position size, market conditions, and execution strategy. The analysis assumes institutional-quality execution, which may not be achievable for all investors.

Fourth, the analysis focuses on U.S. equity factors. While robustness tests confirm that patterns are present internationally, the state-conditioned strategy is calibrated to U.S. data and may require adaptation for other markets.

9.6 Directions for Future Research

Several extensions merit further investigation.

First, the economic mechanisms proposed in Section 7 could be tested more directly using data on funding conditions, arbitrageur positions, and market microstructure. High-frequency data around crash episodes would be particularly informative.

Second, the path-state framework could be extended to other asset classes. Fixed-income factors, currency carry, and commodity momentum may exhibit similar state dependence, and cross-asset path states could provide additional information.

Third, the relationship between path states and option-implied information deserves exploration. The options market may contain forward-looking signals about path dynamics that could improve regime classification.

Fourth, the implications for equilibrium asset pricing could be formalized. A model with heterogeneous agents facing differential funding constraints could generate the state-dependent premia documented here.

9.7 Concluding Remarks

The central message of this paper is that how volatility arrives matters for factor investing. Two markets with identical volatility levels can have profoundly different implications for factor returns, depending on whether volatility formed through a sudden spike or gradual accumulation. By conditioning on the path of volatility formation, investors can avoid the worst factor crashes and achieve more repeatable performance.

This perspective reframes factor premia as compensation for path-conditional risk. The unconditional factor premium is a weighted average across market regimes, including periods of large losses. Investors who can identify path states in real time—or who have longer horizons and greater tolerance for drawdowns—can capture higher risk-adjusted returns by understanding not just how volatile markets are, but how they got there.

References

Ang, A., Hodrick, R. J., Xing, Y., & Zhang, X. (2006). The cross-section of volatility and expected returns. *The Journal of Finance*, 61(1), 259–299.

Arnott, R. D., Beck, N., Kalesnik, V., & West, J. (2016). How can "smart beta" go horribly wrong? *Research Affiliates Working Paper*.

Asness, C. S., Moskowitz, T. J., & Pedersen, L. H. (2013). Value and momentum everywhere. *The Journal of Finance*, 68(3), 929–985.

Asness, C. S., Chandra, S., Ilmanen, A., & Israel, R. (2017). Contrarian factor timing is deceptively difficult. *The Journal of Portfolio Management*, 43(5), 72–87.

Asness, C. S., Frazzini, A., & Pedersen, L. H. (2019). Quality minus junk. *Review of Accounting Studies*, 24(1), 34–112.

Barroso, P., & Santa-Clara, P. (2015). Momentum has its moments. *Journal of Financial Economics*, 116(1), 111–120.

Boguth, O., Carlson, M., Fisher, A., & Simutin, M. (2011). Conditional risk and performance evaluation: Volatility timing, overconditioning, and new estimates of momentum alphas. *Journal of Financial Economics*, 102(2), 363–389.

Bollerslev, T. (1986). Generalized autoregressive conditional heteroskedasticity. *Journal of Econometrics*, 31(3), 307–327.

Brunnermeier, M. K., & Pedersen, L. H. (2009). Market liquidity and funding liquidity. *The Review of Financial Studies*, 22(6), 2201–2238.

Carhart, M. M. (1997). On persistence in mutual fund performance. *The Journal of Finance*, 52(1), 57–82.

Cederburg, S., O'Doherty, M. S., Wang, F., & Yan, X. S. (2020). On the performance of volatility-managed portfolios. *Journal of Financial Economics*, 138(1), 95–117.

Chordia, T., Subrahmanyam, A., & Tong, Q. (2014). Have capital market anomalies attenuated in the recent era of high liquidity and trading activity? *Journal of Accounting and Economics*, 58(1), 41–58.

Daniel, K., & Moskowitz, T. J. (2016). Momentum crashes. *Journal of Financial Economics*, 122(2), 221–247.

Daniel, K., Hirshleifer, D., & Subrahmanyam, A. (2012). Overconfidence, arbitrage, and equilibrium asset pricing. *The Journal of Finance*, 56(3), 921–965.

Engle, R. F. (1982). Autoregressive conditional heteroscedasticity with estimates of the variance of United Kingdom inflation. *Econometrica*, 50(4), 987–1007.

Fama, E. F., & French, K. R. (1989). Business conditions and expected returns on stocks and bonds. *Journal of Financial Economics*, 25(1), 23–49.

Fama, E. F., & French, K. R. (1993). Common risk factors in the returns on stocks and bonds. *Journal of Financial Economics*, 33(1), 3–56.

Fama, E. F., & French, K. R. (2008). Dissecting anomalies. *The Journal of Finance*, 63(4), 1653–1678.

Fama, E. F., & French, K. R. (2015). A five-factor asset pricing model. *Journal of Financial Economics*, 116(1), 1–22.

Frazzini, A., & Pedersen, L. H. (2014). Betting against beta. *Journal of Financial Economics*, 111(1), 1–25.

Frazzini, A., Israel, R., & Moskowitz, T. J. (2018). Trading costs. *Working Paper, AQR Capital Management.*

Gatheral, J., Jaisson, T., & Rosenbaum, M. (2018). Volatility is rough. *Quantitative Finance*, 18(6), 933–949.

Gromb, D., & Vayanos, D. (2010). Limits of arbitrage. *Annual Review of Financial Economics*, 2(1), 251–275.

Guyon, J., & Lekeufack, J. (2023). Volatility is (mostly) path-dependent. *Quantitative Finance*, 23(9), 1221–1258.

Hamilton, J. D. (1989). A new approach to the economic analysis of nonstationary time series and the business cycle. *Econometrica*, 57(2), 357–384.

Harvey, C. R., Liu, Y., & Zhu, H. (2016). ... and the cross-section of expected returns. *The Review of Financial Studies*, 29(1), 5–68.

Hou, K., Xue, C., & Zhang, L. (2015). Digesting anomalies: An investment approach. *The Review of Financial Studies*, 28(3), 650–705.

Hou, K., Xue, C., & Zhang, L. (2020). Replicating anomalies. *The Review of Financial Studies*, 33(5), 2019–2133.

Jagannathan, R., & Wang, Z. (1996). The conditional CAPM and the cross-section of expected returns. *The Journal of Finance*, 51(1), 3–53.

Jegadeesh, N. (1990). Evidence of predictable behavior of security returns. *The Journal of Finance*, 45(3), 881–898.

Jegadeesh, N., & Titman, S. (1993). Returns to buying winners and selling losers: Implications for stock market efficiency. *The Journal of Finance*, 48(1), 65–91.

Koijen, R. S., & Yogo, M. (2018). A demand system approach to asset pricing. *Journal of Political Economy*, 127(4), 1475–1515.

Lettau, M., & Ludvigson, S. (2001). Resurrecting the (C)CAPM: A cross-sectional test when risk premia are time-varying. *Journal of Political Economy*, 109(6), 1238–1287.

Liu, F., Tang, X., & Zhou, G. (2019). Volatility-managed portfolios revisited. *Working Paper, Washington University in St. Louis.*

McLean, R. D., & Pontiff, J. (2016). Does academic research destroy stock return predictability? *The Journal of Finance*, 71(1), 5–32.

Moreira, A., & Muir, T. (2017). Volatility-managed portfolios. *The Journal of Finance*, 72(4), 1611–1644.

Morel, R., Mallat, S., & Bouchaud, J.-P. (2024). Path shadowing Monte Carlo. *Quantitative Finance*, 24(9), 1199–1225.

Novy-Marx, R. (2013). The other side of value: The gross profitability premium. *Journal of Financial Economics*, 108(1), 1–28.

Novy-Marx, R., & Velikov, M. (2019). Comparing cost-mitigation techniques. *Financial Analysts Journal*, 75(1), 85–102.

Santos, T., & Veronesi, P. (2006). Labor income and predictable stock returns. *The Review of Financial Studies*, 19(1), 1–44.

Shleifer, A., & Vishny, R. W. (1997). The limits of arbitrage. *The Journal of Finance*, 52(1), 35–55.

Shumway, T. (1997). The delisting bias in CRSP data. *The Journal of Finance*, 52(1), 327–340.

Stambaugh, R. F., & Yuan, Y. (2017). Mispricing factors. *The Review of Financial Studies*, 30(4), 1270–1315.

A   Detailed Factor Definitions

This appendix provides detailed definitions for all factor signals used in the paper.

A.1   Momentum

The momentum signal for stock i at the end of month t is the cumulative return from month $t - 12$ through month $t - 2$:

$$\text{MOM}_{i,t} = \prod_{s=t-12}^{t-2} (1 + r_{i,s}) - 1 \tag{54}$$

Data requirements:

- At least 8 non-missing monthly returns during the formation period

- Stock price above \$1 at portfolio formation

- Market capitalization above the 20th percentile of NYSE stocks

Portfolio construction:

- Sort stocks into deciles using NYSE breakpoints

- Value-weight stocks within each decile

- Long top decile (past winners), short bottom decile (past losers)

- Rebalance monthly

A.2   Value

The value signal for stock i at the end of month t is the book-to-market ratio:

$$\text{VAL}_{i,t} = \frac{\text{BE}_{i,\tau}}{\text{ME}_{i,t-6}} \tag{55}$$

where $\text{BE}_{i,\tau}$ is book equity for the fiscal year ending in calendar year $\tau = t - 18$ months (approximately) and $\text{ME}_{i,t-6}$ is market equity at the end of June.

Book equity definition:

$$\text{BE} = \text{SEQ} + \text{TXDITC} - \text{PS} \tag{56}$$

where:

- SEQ = Stockholders' equity (Compustat item `SEQ`)

- TXDITC = Deferred taxes and investment tax credit (`TXDITC`)

- PS = Preferred stock (redemption value `PSTKRV`, or liquidating value `PSTKL`, or par value `PSTK`)

Timing convention:

- Use book equity from fiscal year ending in calendar year $t - 1$

- Match with market equity from December of year $t - 1$

- Form portfolios at the end of June of year t

- Hold portfolios from July of year t through June of year $t+1$

  Data requirements:

- Positive book equity

- Non-missing market equity

- At least 6-month lag between fiscal year end and portfolio formation

A.3 Quality (Gross Profitability)

The quality signal for stock i at the end of month t is gross profitability:

$$\text{QUAL}_{i,t} = \frac{\text{REVT}_{i,\tau} - \text{COGS}_{i,\tau}}{\text{AT}_{i,\tau}} \tag{57}$$

where:

- REVT = Total revenue (Compustat item `REVT`)

- COGS = Cost of goods sold (`COGS`)

- AT = Total assets (`AT`)

  Timing convention:

- Same as value factor

- Use accounting data from fiscal year ending in calendar year $t-1$

- Form portfolios at the end of June of year t

  Data requirements:

- Non-missing revenue, cost of goods sold, and total assets

- Positive total assets

- Exclude financial firms (SIC codes 6000–6999)

A.4 Low Risk (Beta)

The low-risk signal for stock i at the end of month t is the negative of estimated market beta:

$$\text{LVOL}_{i,t} = -\hat{\beta}_{i,t} \tag{58}$$

where $\hat{\beta}_{i,t}$ is estimated from:

$$r_{i,s} - r_{f,s} = \alpha_i + \beta_i(r_{m,s} - r_{f,s}) + \varepsilon_{i,s} \tag{59}$$

using monthly returns over months $s \in \{t-60, \ldots, t-1\}$.

  Data requirements:

- At least 36 non-missing monthly returns during the estimation period

- Winsorize estimated betas at the 1st and 99th percentiles

  Portfolio construction:

- Sort stocks into deciles using NYSE breakpoints

- Value-weight stocks within each decile

- Long bottom decile (low beta), short top decile (high beta)

- Rebalance monthly

B   Path State Construction Details

This appendix provides additional details on the construction of path state variables and regime classification.

B.1   Realized Volatility Computation

Realized volatility over horizon h is computed as:

$$\sigma_t^{(h)} = \sqrt{\frac{252}{n_h} \sum_{i=0}^{n_h-1} r_{t-i}^2} \tag{60}$$

where r_{t-i} is the daily market return on day $t-i$ and n_h is the number of trading days in horizon h:

- $h = 1\text{w}$: $n_h = 5$ trading days

- $h = 1\text{m}$: $n_h = 21$ trading days

- $h = 3\text{m}$: $n_h = 63$ trading days

- $h = 6\text{m}$: $n_h = 126$ trading days

The factor of 252 annualizes the volatility estimate (assuming 252 trading days per year).

B.2   Volatility Ratio

The volatility ratio is:

$$\rho_t^\sigma = \frac{\sigma_t^{(1\text{w})}}{\sigma_t^{(3\text{m})}} \tag{61}$$

Interpretation:

- $\rho_t^\sigma > 1$: Short-term volatility exceeds long-term volatility (volatility increasing)

- $\rho_t^\sigma \approx 1$: Volatility stable across horizons

- $\rho_t^\sigma < 1$: Short-term volatility below long-term volatility (volatility decreasing)

B.3 Drawdown Measures

The drawdown magnitude is:

$$\mathrm{DD}_t = \frac{\max_{s \in [t-126,t]} P_s - P_t}{\max_{s \in [t-126,t]} P_s} \tag{62}$$

expressed as a percentage decline from the trailing 6-month high.

The drawdown duration is:

$$\tau_t = t - \arg \max_{s \in [t-126,t]} P_s \tag{63}$$

measured in trading days.

The drawdown speed is:

$$\mathrm{Speed}_t = \frac{\mathrm{DD}_t}{\tau_t} \times 21 \tag{64}$$

expressed as percentage decline per month (scaled by 21 trading days).

B.4 Regime Classification Algorithm

The regime classification proceeds as follows:

1. **Compute state variables**: At the end of each month t, compute $\sigma_t^{(1m)}$, ρ_t^σ, DD_t, and Speed_t using daily data through month t.

2. **Estimate quantile thresholds**: Using data from the start of the sample through month $t-1$, estimate the 33rd and 67th percentiles of the historical distribution of $\sigma^{(1m)}$:

$$Q_{0.33,t} = \mathrm{Percentile}_{0.33} \left(\sigma_1^{(1m)}, \ldots, \sigma_{t-1}^{(1m)} \right) \tag{65}$$

$$Q_{0.67,t} = \mathrm{Percentile}_{0.67} \left(\sigma_1^{(1m)}, \ldots, \sigma_{t-1}^{(1m)} \right) \tag{66}$$

3. **Classify volatility level**:

   - Low: $\sigma_t^{(1m)} \leq Q_{0.33,t}$
   - Medium: $Q_{0.33,t} < \sigma_t^{(1m)} \leq Q_{0.67,t}$
   - High: $\sigma_t^{(1m)} > Q_{0.67,t}$

4. **Classify volatility dynamics** (for high-volatility states only):

   - Spike: $\rho_t^\sigma > 1.5$
   - Sustained: $0.8 \leq \rho_t^\sigma \leq 1.5$
   - Decaying: $\rho_t^\sigma < 0.8$

5. **Assign regime**:

   - Calm Trend: Low volatility
   - Choppy Transition: Medium volatility
   - Slow-Burn Stress: High volatility, Sustained dynamics
   - Crash-Spike: High volatility, Spike dynamics
   - Recovery: High volatility, Decaying dynamics

Table 38: Regime Transition Probabilities

From \ To	Calm	Choppy	Slow-Burn	Crash-Spike	Recovery
Calm Trend	0.82	0.15	0.02	0.01	0.00
Choppy Transition	0.18	0.68	0.08	0.04	0.02
Slow-Burn Stress	0.02	0.12	0.72	0.08	0.06
Crash-Spike	0.00	0.05	0.25	0.45	0.25
Recovery	0.08	0.22	0.15	0.05	0.50

Notes: Table reports the probability of transitioning from each regime (rows) to each other regime (columns) over a one-month horizon. Sample period is January 1963 to December 2023.

B.5 Regime Transition Matrix

Table 38 reports the empirical transition probabilities between regimes.

Key observations:

- Calm Trend and Slow-Burn Stress are the most persistent regimes (82% and 72% self-transition probabilities)

- Crash-Spike is the least persistent regime (45% self-transition probability)

- Crash-Spike transitions primarily to Slow-Burn Stress (25%) or Recovery (25%)

- Direct transitions from Calm Trend to Crash-Spike are rare (1%)

C Additional Robustness Tables

C.1 Industry-Neutral Factor Performance

Table 39 reports state-conditional performance for industry-neutral factor portfolios.

Table 39: State-Conditional Performance: Industry-Neutral Factors

	Calm	Choppy	Slow-Burn	Crash-Spike	Recovery
Mean Monthly Returns (%)					
Momentum	1.18	0.62	0.15	-2.95	0.78
Value	0.32	0.28	0.42	-0.58	1.05
Quality	0.28	0.22	0.38	0.55	0.15
Low-Risk	0.15	0.12	0.25	0.32	-0.08
State-Conditioned Strategy Sharpe Ratio					
Momentum			0.52		
Value			0.28		
Quality			0.38		
Low-Risk			0.28		

Notes: Industry-neutral factors sort stocks within each of 48 Fama-French industries and take long-short positions within industries. Sample period is January 1963 to December 2023.

Industry-neutral factors exhibit similar state-conditional patterns to unrestricted factors, though with smaller magnitudes. Momentum losses in Crash-Spike states are -2.95% (vs. -3.85% unrestricted), suggesting that approximately one-quarter of momentum's crash exposure comes from industry bets.

C.2 Quintile-Based Factors

Table 40 reports state-conditional performance for quintile-based (rather than decile-based) factor portfolios.

Table 40: State-Conditional Performance: Quintile-Based Factors

	Calm	Choppy	Slow-Burn	Crash-Spike	Recovery
Mean Monthly Returns (%)					
Momentum	1.15	0.58	0.12	-3.25	0.72
Value	0.32	0.28	0.45	-0.65	1.08
Quality	0.28	0.22	0.38	0.58	0.15
Low-Risk	0.18	0.14	0.28	0.35	-0.10

Notes: Quintile-based factors sort stocks into five groups (rather than ten) and go long the top quintile and short the bottom quintile. Sample period is January 1963 to December 2023.

Quintile-based factors show similar patterns with slightly smaller magnitudes, reflecting the less extreme sorting.

C.3 Performance by Decade

Table 41 reports unconditional and state-conditioned momentum performance by decade.

Table 41: Momentum Performance by Decade

Decade	Unconditional		State-Conditioned	
	SR	MaxDD	SR	MaxDD
1963–1969	0.45	28.5%	0.52	22.8%
1970–1979	0.38	35.2%	0.48	25.5%
1980–1989	0.62	22.5%	0.68	18.2%
1990–1999	0.85	18.8%	0.88	15.5%
2000–2009	-0.05	68.2%	0.35	32.5%
2010–2019	0.42	25.8%	0.58	18.5%
2020–2023	0.28	28.5%	0.52	15.2%

Notes: SR = Sharpe Ratio. MaxDD = Maximum Drawdown.

State conditioning improves performance in all decades, with the largest improvements in the 2000s (which includes the 2008–2009 momentum crashes) and the 2020s (which includes the March 2020 crash).

D Variable Definitions

Table 42: Variable Definitions

Variable	Definition
Return Variables	
$r_{i,t}$	Monthly holding-period return on stock i in month t, including dividends
r_t^f	Monthly return on factor f (long-short decile portfolio)
r_t^m	Monthly return on the value-weighted market portfolio
r_t^{rf}	One-month Treasury bill rate
Firm Characteristics	
$\mathrm{ME}_{i,t}$	Market equity: price times shares outstanding at end of month t
$\mathrm{BE}_{i,t}$	Book equity: stockholders' equity plus deferred taxes minus preferred stock
$\mathrm{B/M}_{i,t}$	Book-to-market ratio: BE/ME
$\mathrm{GP}_{i,t}$	Gross profitability: (revenue − COGS) / total assets
$\beta_{i,t}$	Market beta: slope from regression of excess returns on market excess returns
Path State Variables	
$\sigma_t^{(h)}$	Realized volatility over horizon h, annualized
ρ_t^σ	Volatility ratio: $\sigma_t^{(1w)}/\sigma_t^{(3m)}$
DD_t	Drawdown: percentage decline from trailing 6-month high
Speed_t	Drawdown speed: drawdown divided by duration
s_t	Path state vector: $(r_t^{(1m)}, r_t^{(3m)}, \sigma_t^{(1w)}, \sigma_t^{(1m)}, \sigma_t^{(3m)}, \sigma_t^{(6m)}, \rho_t^\sigma, \mathrm{DD}_t, \mathrm{Speed}_t)$
Performance Metrics	
SR	Sharpe ratio: mean excess return divided by standard deviation, annualized
MaxDD	Maximum drawdown: largest peak-to-trough decline
IC	Information coefficient: cross-sectional correlation of signal and subsequent return